EXPERIMENTAL INVESTIGATIONS OF IMPROVING BUSHING QUALITY AND JOINING SHEET METALS IN FRICTION DRILLING

A Thesis

by

KUAN-YU SU

Submitted to the Office of Graduate and Professional Studies of
Texas A&M University
in partial fulfillment of the requirements for the degree of

MASTER OF SCIENCE

Chair of Committee,	Jyhwen Wang
Committee Members,	Michael Johnson
	Xinghang Zhang
Head of Department,	Andreas Polycarpou

May 2015

Major Subject: Mechanical Engineering

ABSTRACT

Friction drilling is a novel hole-making process performed on thin-walled sheet metals. The friction between a rapid-rotating conical tool and a sheet metal generates heat to soften the work material and penetrate it to form a hole. The bushing is formed in situ from the workpiece.

This experimental study investigated friction drilling process. Axial thrust forces during the process were measured by a dynamometer and data acquisition system. The thrust force curves and the cross-sectioned images of friction-drilled holes were characterized to study the effects of process parameters such as spindle speed, feed rate, workpiece thickness, and tool diameter. The results showed that either increasing spindle speed or decreasing feed rate can reduce the thrust forces.

Generating a bushing with good quality has been a challenge in friction drilling. The lower die fixture was designed to improve the bushing shape in its cylindricality, cracks and petal formation. Threads were tapped to demonstrate the improvement of the bushing quality in practical application.

Due to the similarities in friction stir welding and friction drilling, the feasibility of joining sheet metals in friction drilling was explored. Different coalescence conditions were observed. The potential of joining sheet metals by friction drilling was demonstrated.

ACKNOWLEDGEMENTS

I would like to express the sincerest appreciation to my advisor, Professor Jyhwen Wang, for being a colossal mentor for me. With your insightful advices and guidance, I have learned and improved to be able to complete my master degree. Your encouragement academically and mentally helps me a lot in my research as well as my career.

I would also like to thank my committee members, Professor Michael Johnson and Professor Xinghang Zhang for your guidance and assistance. I thank Frank Cervantez and Adams Farmer for authorizing and instructing me to operate various machines and tools.

A special gratitude is conveyed to my beloved family for their financial support and unfailing encouragement. I also appreciate the help and suggestions from my lab colleges: Cheng-Kang Yang, Bright Wadja, Ying Zhang, Ruoshui Wang, and Han-Hsuan Lin.

TABLE OF CONTENTS

Page

LIST OF FIGURES

Page

LIST OF TABLES

Page

1. INTRODUCTION: FRICTION DRILLING PROCESS AND EXPERIMENT

Friction drilling is a novel hole-making process [1]. The friction between a rapidly rotating conical tool and a sheet metal generates the heat to deform the work material and penetrate a hole [2, 3]. Thus, the process is also known as flow drilling, thermal drilling, form drilling, or friction stir drilling. The softened work material is pushed sideward and downward to make a bushing directly [4]. All work-materials deformed from the friction drilled hole contribute to the forming of boss and bushing. The length of the bushing is up to three times thick as the original workpiece. The additional thickness provides more strength and support than original sheet to thread the hole. The technique to form bushing on the thin-walled workpiece, sheet metal, or tube makes it simple to joint devices efficiently. The requirement for attaching devices to thin-walled workpieces in current industry processes such as drilling a hole, attaching a chip, and welding a nut is efficiently replaced by one step, friction drilling.

Different from the traditional drilling process requiring the cutting fluid to remove chips and the heat, friction drilling is a dry and clean process. The reshaping instead of cutting process makes it a chipless operation [5]. On occasion, a small amount of lubricant is applied in order to reduce adhesion of the workpiece material to the surface of the friction drill bit. The lubricant pasted results in longer tool lifetime, and better quality of the inner surface of the bushing [6].

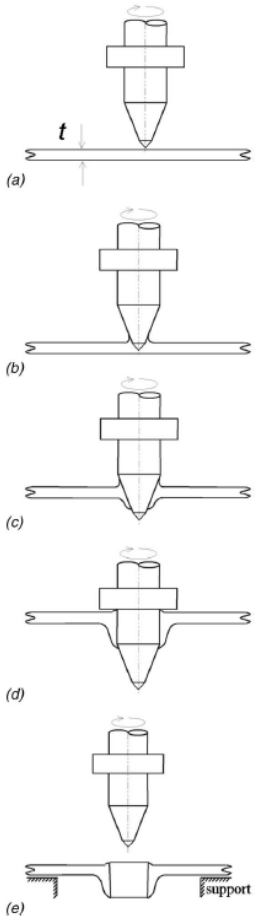

Figure 1: Schematic illustration of the friction drilling process [7].

The schematic illustration of friction drilling process is shown in Figure 1. The conical tool approaches and makes contact with the top surface of the workpiece, as shown in Figure 1(a). With high axial force and rotational speed, the heat generated by the friction from axial thrust forces and torques softens the work material as the tip of the conical part extrudes into the workpiece, as shown in Figure 1(b). As the work material reaches the plastic deformation criterion, the softened and malleable workpiece

material is pushed upward and sideward. Once it surpasses the yielding point, the tool penetrates the workpiece. The tool keeps traveling to displace the material upward to form the boss around the upper surface of the workpiece. The material flowing beneath forms the bushing in the lower surface of the workpiece with the cylindrical part of the friction drill bit, as shown in Figure 1(c). The shoulder part of the tool may have contact with the back-extruded material, also known as boss, to modify the burr in various fashions, as shown in Figure 1(d). The standard type friction drill tool rolls over the up-flowing material, whereas the flat type friction drill tool shear the boss to produce a flush surface. Finally, the friction drill tool retracts, and completes a hole-drilling process, as shown in Figure 1(e).

The friction drilling process takes various advantages over traditional approaches of attaching devices to thin-walled workpieces or sheet metals. Pre-hole and burring are not the requirement, however, it is necessary for weld nut and rivet nut process. In terms of manufacturing process, it is dry and clean for friction drilling without using cutting fluid and generating chips. The error rate caused by the tendency of deviation is relatively low. Friction drilled holes have homogeneous microstructure of joining, while the partly-joined nut welding or riveting does not. Therefore, the friction drilled holes is highly reliable, and have higher torque loading capability [8].

Although some researches about friction drilling have previously been done, some open issues are still needed to be studied. First, a more detailed and comprehensive fundamental parameters analysis in friction drilling is needed. Previous researches looked into the effects of different parameters, such as spindle speed, feed rate,

workpiece thickness, and drill bit diameter on the thrust force. However, the understanding of the effect of various parameters on the forces and the geometries of the hole is not adequate. The combination effect on the thrust force has not been investigated. A more thorough parametric study is essential to achieve a better understanding of different input parameters in friction drilling.

One of the focuses in this research is to experimentally investigate the parameters which affect the axial thrust forces during friction drilling process. The parameters studied are spindle speed and feed rate of the friction drill bit, the thickness of the workpiece, and the diameter of the friction drill bit. The combination effect of spindle speed and feed rate on the thrust forces is investigated. Experiments are conducted to measure and collect the forces when friction drilling the work material in different conditions. The samples of the friction drilled holes are examined to characterize the feature of the bushing shapes.

Another objective of the research is to improve the quality of the friction drilled holes as the previous work had not paid much attention to the improvement of the hole quality. Pre-heating [9] and pre-drilling [10] methods are the only two approaches investigated to achieve the goal of obtaining better hole quality previously. However, the longer processing time and some derivative problems become the obstacles of the friction drilling process. A novel approach with the aim to improve the hole quality is introduced in the present work. The approach is to carry on the friction drilling process with a designed lower die which is able to control the bushing to a desired shape. The geometry of the cavity of the lower die is expected to play an important role in forming

the bushing shape. The axial thrust forces are measured and the geometries of the bushing shapes are also characterized. Furthermore, the threads are tapped in the friction drilled hole to assess the performance of the improved holes.

The friction drilled holes are often created and tapped to join devices to thin-walled workpieces. Inspired by friction welding process, it may be possible to joint two thin-walled devices using friction drilling directly without applying a fastener. Another focus of the research is to conduct an in-depth investigation of joining sheet metals using friction drilling.

2. LITERATURE REVIEW

2.1 Introduction

In the stone-age time, the behavior of rubbing two objects to generate heat and fire is recorded. However, to apply the technique to drill holes in metal workpieces is developed in more recent decades. Due to its primeval stage in manufacturing, researches and publications on the topic of friction drilling are limited. Six patents related to friction drilling operation of early stage by van Geffen in 1970s [2-4, 11] and later by Head et al. [12] and Hoogenboom [13] in 1980s have been issued. France et al. [14, 15] did research in strength and rotational stiffness of the friction drilled holes using metal tubing. Overy [16] studied the bushing formation of the friction drilled holes in the designing perspective. Streppel and Kals [1] executed the different input parameters in flow drilling and analyzed the results mechanically and physically. Kerkhofs et al. [17] researched the performance of uncoated flow drill bit comparing with (Ti,Al)N coated flow drill bit.

Previous research related to friction drilling is discussed in the section. Four categories including force analysis, bushing shape investigation, microscopic observation, and fundamental finite element analysis show the frame of the research in friction drilling.

2.2 Force analysis

Streppel and Kals published a preliminary analysis of friction drilling in the perspective of mechanical and physical. The force curve of friction drilling is first of found in the paper. The characteristics of the thrust force and feed velocity are plotted in solid line and dashed line, respectively, against the tool travel distance in z direction.

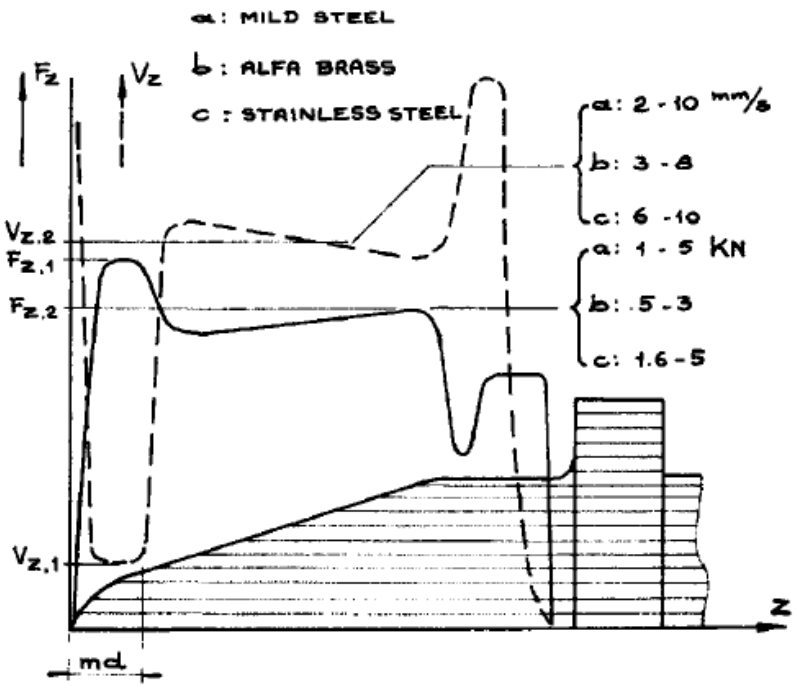

Figure 2: The force and velocity curve in friction drilling.

A preliminary study of the thrust forces and torques has been studied by Miller et al. [9] The cast aluminum and magnesium alloys workpieces are experimented in the study. To avoid bushing with radial fracture, pre-heating the workpiece and higher spindle speed are conducted. As the workpiece temperature increased, the thrust force and the torque both apparently decrease, and the shape of bushing was improved. To verify the benefits, the energy, peak power, and average power were analyzed. [9] The recorded torques was noticed varying, due to the adhesion wear from the workpiece to the drill bit. High affinity of aluminum to the tool is known [18].

2.3 Shape of bushing and hole quality

The bushing shape and the hole depth are two important criteria to evaluate the quality of holes in friction drilling. The shape of bushing is observed and judged via cylindricality, cracks, and petal formation.

Crack and petal formation are both undesirable for the thread inside the drilled holes. They are poor traits of bushing due to low ductility of material. Observed by experiments, the number of petals is related to the ratio of the workpiece thickness t and the drill bit diameter d. With the same spindle speed and feed rate, the shape of bushing becomes more ideal and cylindrical, as the workpiece temperature raises. The quality of the bushing has nothing to do with feed rates experimentally.

The change of spindle speed has no big effect on bushing shape in Al 380 at room temperature. There are still significant crack and petal formation at highest spindle speed. However, spindle speed has negative effects on bushing shape in MgAZ91D. At

highest spindle speed, 15000 rpm, evident petal formation even layered one is observed which is similar to the bushing shape at room temperature in Al 380. It concluded that the brittle cast metal was less appropriate than ductile sheet metal in friction drilling due to improper bushing shape exhibiting cracks or petal formation [9].

The friction drilled hole geometry was investigated experimentally in AISI 1010 steel square-tube material. The geometry including the washer (boss) geometry, the height of bushing, and the petal geometry was examined with respect to different spindle speeds and feed rates. The experimental results showed the washer (boss) geometry was improved by increasing spindle speeds, and thus the height of bushing is extended. The decrease in radial forces caused by the increase of spindle speeds made sure the smoother washer (boss) was created because of less effect on washer geometry. With high feed rates, the geometry of washer (boss) and the bushing was distorted. For the reason, the low temperature caused by the increased thrust forces in high feed rates effects the washer geometry on the increased ruptures. In the analysis of the bushing shape, the bushing length, petals, and the bushing hemlines are investigated. As the spindle speed increases, the bushing length extends, and less petal formation at the bushing hemline is examined. Compared to the spindle speed effect, the effect of feed rate on the bushing length is small. Nevertheless, the bushing length is found reduced in the high feed rate operation. At the lower hole zone temperature, the deformation hardening on the workpiece is caused by the rapid deformation in the high feed rate condition. Therefore, the extrusion length reduces, and more petals are generated [19].

Pre-drilling friction drilling was investigated as a novel method for improving the bushing shape using A7075-T651 aluminum alloy, which is a brittle cast material. Due to less contact area between the tool and work material, pre-drilling technique caused less temperature increase. Thus, for compensating the temperature deficiency in pre-drilling friction drilling process, higher spindle speed and lower feed rate are inevitable to gain more rotational cycles for generating more friction heat.

With the preferred spindle speed and feed rate, the surface roughness decreased as the diameter of the pre-drilling hole increased. To judge the quality of bushing shape, the cracks and petal formation were observed eliminated in pre-drilling friction drilling process. With the larger pre-drilling diameter, the shape of bushing including cylindricality, cracks, and petal formation were improved [10].

2.4 Microscopic alternations

In friction drilling process, the high temperature and huge deformation are occurred. The alternations in microstructures and material properties of the workpieces are predictable. Miller et al. characterized the microstructural alternations and subsurface micro indentation hardness changes in friction drilling using the materials of steel, aluminum, and titanium [20]. Figure 3 shows the damages in the inside surface of the friction drilled hole using Al 5052 as the work material. The image shows the evidences of extensive plastic deformation, abrasion and scored trait.

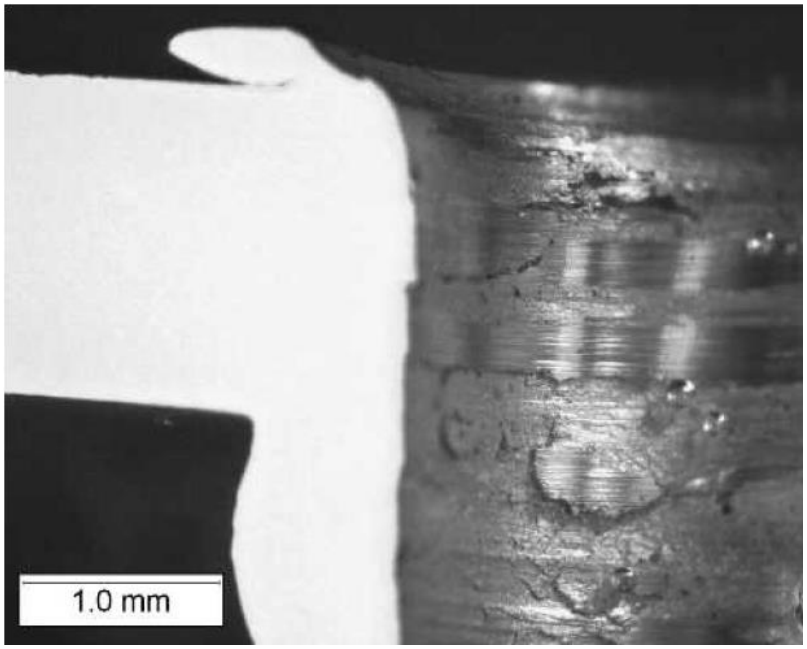

Figure 3: The inside part of the friction drilled hole in Al 5052 metal sheet.

Chow et al. addressed that the finer grain size and compact structure with large micro-hardness is observed near to the friction drilled area [21]. Contrarily, the locations away from the drilled hole contain coarser grain size and low micro-hardness.

2.5 Finite element analysis

A similar process, friction stir welding (FSW) has been simulated by the finite element method utilizing the ABAQUS/Explicit [22-24]. Both processes generate frictional heat by rotating tools. The difference is that friction drilling deforms material to make a hole, while friction stir welding joins work materials. Modeling is necessary to understand stresses, strains, temperatures, and the material flow. Miller et al.

investigated the 3D finite element modeling using ABAQUS/Explicit. The validation was made by comparing the thrust forces and torques of modeling results to experimental measurements [25].

The simulation of the deformation occurring in friction drilling process is a temperature-dependent non-linear problem [26]. High speed rotating tool travels at constant velocity into the sheet metal generating high temperature produces huge deformation of the work material. The process of the friction drilling involves high complexity of friction behavior and contact interaction. The two simulation methods, ABAQUS/Explicit and ABAQUS/Implicit, are adequate for modeling [25, 27].

The ABAQUS/Implicit method solves non-linear problems with implicit time integration and iterative global stiffness matrix. The implicit method is mostly satisfactory for the dynamic problems with accurate iterative solution. However, the large consumption of computational time and memory is needed. The ABAQUS/Explicit was applied in this study to simulate the thermal and mechanical process in friction drilling. An explicit dynamics finite element method is selected to deal with large plastic strain, high temperature workpiece deformation, as well as complex interactions between tool and work-material. ABAQUS/Explicit enables to analyze types of problems, such as large, nonlinear, quasi-static analyses, high-speed dynamics, and coupled temperature-displacement [27]. The advantages are: It is designed to solve discontinuous, dynamic problems efficiently. It saves more disk space for large problems. It is capable of simulating quasi-static problems easily.

2.6 Scope of research

Although some researches about friction drilling have previously been done, there are still a plenty of issues needed to be addressed. The primary objective of the research is to provide broader and deeper knowledge of the non-traditional hole-making process called friction drilling.

The scope of research consists of fundamental parameters study in thrust force curves, improvement of the bushing shape, investigation of joining sheet metals by friction drilling, and some observations associated with bushing shapes. Detailed topics and approaches are addressed in the following sections.

2.6.1 Fundamental parameters analysis in friction drilling process

The complete investigation of thrust force and torque based on various parameters in the friction drilling process has not been conducted. The goal of the study is to measure and then characterize the axial forces and torques with different variables. Experiments are carried out using a Bridgeport computer numerically controlled (CNC) milling machine. The data of thrust forces and torque are recorded during friction drilling process by data acquisition system. Different variables are involved, such as spindle speeds and feed rates of the tool, thickness and number of workpieces, diameter of the tool. With these parameters, the characterization and the explanation of the curves are more comprehensive and convincing [28].

2.6.2 Improvement of the bushing shape

Friction drill bit has been designed to satisfy certain bushing shapes [11]. However, the shape of bushing is one of the important criteria to evaluate the quality of the friction drilling hole [9]. Though some observations of the bushing shape have been made by Miller, the practical improvement of the shape of bushing is still an unanswered problem. The novel design of the fixture of the workpiece is executed. The goal of the study is to improve the quality of the hole in order to provide more strength and effective length for threading. Parametric study is also conducted in the section.

2.6.3 Joining process in friction drilling

Double-layered workpieces in friction drilling experiment with the original fixture is investigated. The potential of joining sheet metals by friction drilling process is demonstrated. Parametric study and friction drilled hole cross section observation are conducted as well. The designed lower die is then applied to investigate the influence on work materials.

3. EXPERIMENTAL SETUP

3.1 Introduction

The section describes the components of the experimental setup including the experiment of the friction drilling process and the measurement of force data. The selected three-axis computer numerical control (CNC) milling machine, friction drill bits, and designed fixture which are necessary components for the friction drilling experiment are presented. In addition, the detail description of the data acquisition system for the force analysis is shown.

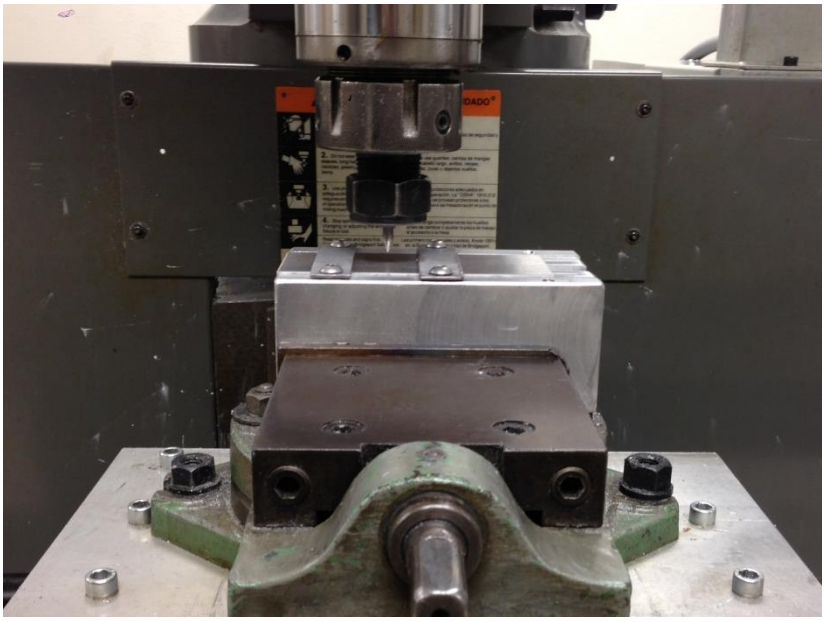

Figure 4: Basic components for friction drilling experiment.

Figure 4 shows the essential components to perform friction drilling process. The basic components needed include the Bridgeport three-axis computer numerical control (CNC) machine, friction drilling tool, sheet metal workpiece, and the fixture to securely hold the workpiece.

3.2 Machine & fixture

A Bridgeport three-axis computer numerical control (CNC) milling machine is used for the experiment of friction drilling. The CNC milling machine has the capability of 4000 rpm maximum spindle speed about z axis which is appropriate for friction drilling experiment.

A fixture to hold the workpiece is designed and machined. The fixture is necessary to fix the workpiece securely when the friction drilling process is operated. The workpiece is clamped by the bolts and bars in the shallow step of 0.076 cm. The deep slot is machined in the center of the fixture. The slot is 1.27 cm width by 2.54 cm depth which allows sufficient clearance between the drill bit and the fixture when the hole is penetrated. This fixture is mounted on the dynamometer on the CNC milling machine.

3.3 Workpiece

Two different workpieces are used in the experiment. The material thicknesses of 1.25 mm and 2.29 mm are selected for friction drilling.

The workpiece material selected is aluminum alloy 6061-T651. The material is widely used in automotive industry, and is suggested for friction drilling process, due to the characteristics of excellent machinability and good weldability.

3.4 Data acquisition system

To measure the forces in the three principal directions, the measurement starts with a dynamometer. The output signal is transferred to the amplifier. The signal converter is required to convert the analog signal to digital signal which is readable for the data acquisition software in the laptop. Detailed descriptions are shown in the following section.

3.4.1 Dynamometer

The AMTI (Advanced Mechanical Technology Inc.) MC818 series dynamometer used in the experiment is the platform-type and multi-component equipment. The dynamometer is bolted on the CNC machine table and the fixture for the sheet metal workpiece is firmly seated on the surface. The model used is capable of measuring 8900 N load, and providing four output channels to measure the forces in X, Y, Z directions, i.e., F_x, F_y, F_z, and the moment about X axis, i.e., M_x. The instrument performs the measurements of force and torque by strain gages. The analog voltage signals which are proportional to actual forces during the friction drilling process are generated and transferred to the amplifier.

3.4.2 Amplifier

The output signals from the dynamometer transfer to the amplifier shown in Figure 5. The sensitivity of the stain gages is in the order of microvolts/volt-unit load. Thus, amplification is necessary to supply high level output signals. The Missile Command Amplifier (Model MCA amplifier) is compatible with AMTI dynamometer. The gain of the amplifier is adjustable by the switches on the panel. The voltage gain in the experiment is 4000.

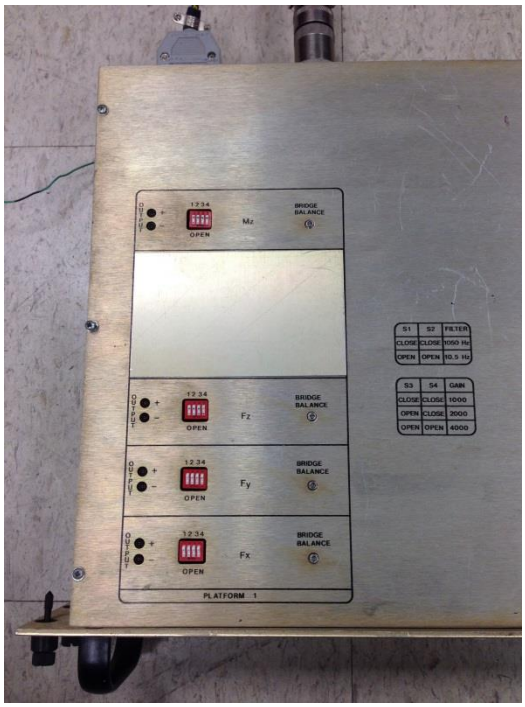

Figure 5: AMTI Missile Command Amplifier.

There are nine distinct wires on the amplifier. Four wires manage the forces in X, Y, Z directions and the moment about X axis. The other five wires are connected to ground. Prior to wire connections, it is required to connect a ground wire to the body of the amplifier for safety purpose. The filters of 10.5 Hz and 1050 Hz are built in the amplifier. The low pass filter removes the undesirable noise in the signal.

To minimize the errors in the measurement, it is important to warm up the amplifier for 30 minutes and balance the amplifier channels before collecting data. After the amplifier system warms up, the potentiometer needs to be properly balanced by using a screw driver. Each amplifier corresponds to a pair of LED light which indicates a positive or negative error when the light is on. While the light on both sides go out, the voltage output ensures zero at the initial stage.

3.4.3 Analog to digital signal converter

The analog to digital signal converter is needed to convert the analog signal from the amplifier into the digital signal captured by data acquisition software. The converter used in the experiment is NI USB-6008 from National Instruments and shown in Figure 6.

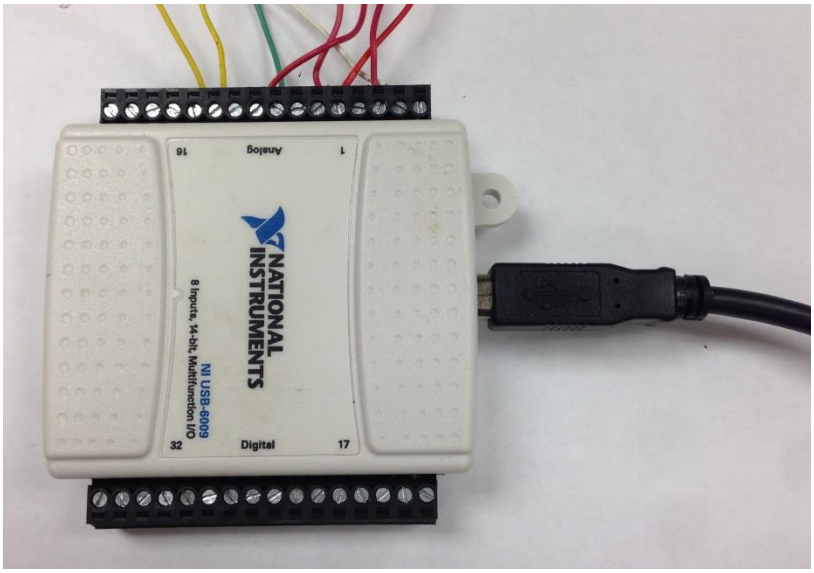

Figure 6: NI USB-6008 analog to digital signal converter.

The connection in differential method is applied. The output wires on the amplifier are connected to the analog side of the converter. The signal value captured by the converter is the difference between the positive and negative ends. The wire which transfers the force signal in X direction is plugged into the port AI2 at the converter analog end which is the positive end in differential method. The ground wire is plugged into port AI3 which is the negative end. By analogy, the positive end from the force signals in Y and Z direction is connected to channel AI5 and AI8 respectively. The corresponding negative end is connected to adjacent channel AI6 and AI9 respectively.

3.4.4 Data acquisition software

After the analog signal from the amplifier is converted into digital signal, it is delivered via Universal Serial Bus, so called USB, to the data acquisition software. The software used in the experiment is LabVIEW SignalExpress LE. During the friction drilling process, the voltage signal is collected and recorded with the selected sampling rate of 1000 Hz. The collected digital voltage signals are then exported to Microsoft Excel. The system calibration is needed to convert the voltage values to the exact force values.

3.5 Friction drilling tool

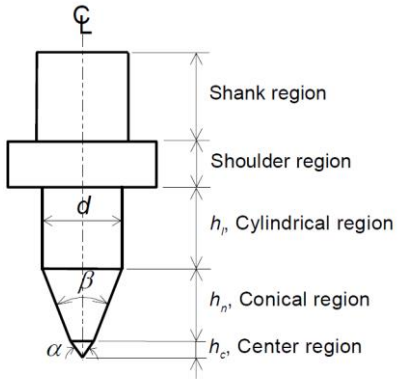

Figure 7: Dimensions and regions of the friction drilling tool [9].

The friction drilling tool provided by Flowdrill© is made of tungsten carbide in cobalt matrix. The Flowdrill© solid tungsten carbide bit is designed for friction drilling

of aluminum, steel, stainless steel, and brass. Two sizes of the friction drilling tool shown in Figure 8 and Figure 9 are used in the experiment.

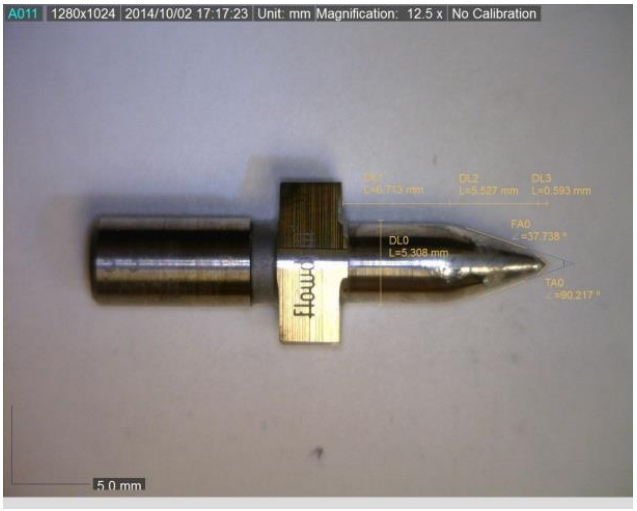

Figure 8: Long Flat 5.3 mm Flowdrill© friction drill bit used in the experiment.

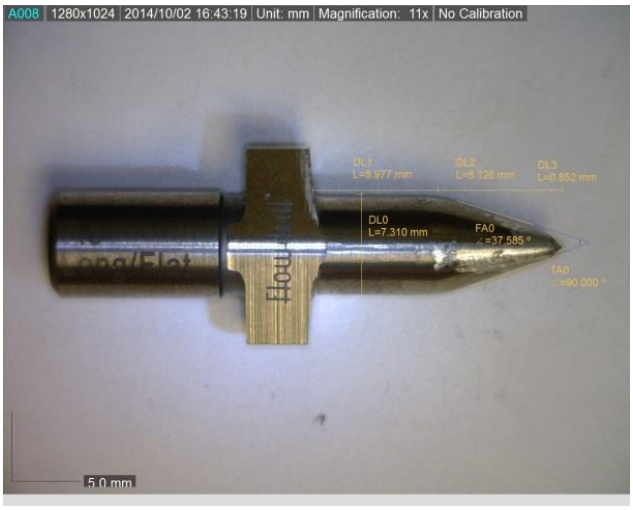

Figure 9: Long Flat 7.3 mm Flowdrill© friction drill bit used in the experiment.

Table 1: Specification of the Flowdrill© friction drilling tools [8]

	Long Flat 5.3 Flowdrill© (FD053LF)	Long Flat 7.3 Flowdrill© (FD073LF)
Material	tungsten carbide	tungsten carbide
Hole size d (mm)	5.3	7.3
Shank diameter (mm)	6.0	8.0
angle α (degree)	90	90
angle β (degree)	38	38
center height h_c (mm) (inch)	0.593 (0.023)	0.852 (0.033)
conical height h_n (mm) (inch)	5.527 (0.217)	8.126 (0.32)
cylindrical height h_l (mm) (inch)	6.713 (0.264)	8.977 (0.353)

The tool geometry is critical to the performance of the bushing shape and drilling process. Five key sections of the tool geometry are shown in Figure 7.

(1) Center part: The angle α and the height h_c are two key parameters of the cone-shaped center. For the initial region to contact the workpiece, its high angle and reduced height generate the larger axial forces and more heat in the beginning. In addition, like the center drill bit in traditional drilling process, the center region spots hole center in order to reduce tendency to wander at the start of drilling.

(2) Conical part: The angle and height in conical part are defined as β and h_n, respectively. The angle β in conical part is sharper than that in center part. In the region, the sheet metal workpiece is softened and then penetrated by frictional

heat and force. As the conical part travels downward, the work-material is gradually pushed sideward to form the bushing.

(3) Cylindrical part: The length and diameter in cylindrical part are defined as h_l and d, respectively. This part configures the complete hole diameter and the bushing shape.

(4) Shoulder part: This part may have contact with the workpiece material to create a finer surface. The boss will be modified in different fashions depending on the standard type or the flat type of friction drilling bit. The flat type which incorporates a milling cutter to provide a smooth, flush top surface to the formed hole is used in the experiment. Therefore, it can also be considered as the chip breaker part.

(5) Shank part: The shank is cylindrical. It allows the tool holder of the spindle to grip the friction drilling tool firmly and tightly.

4. FRICTION FRILLING EXPERIMENT

4.1 Introduction

Friction drilling experiments were conducted in different variables such as spindle speed, feed rate, workpiece thickness, and drill bit diameter. The axial thrust forces were measured and the geometries of the bushing were studied. The dynamometer with fixed Cartesian coordinate system was bolted on the CNC machine table, and the fixture for the sheet metal workpiece was firmly clamped on the surface. The surface normal of the workpiece was set to the Z direction in Cartesian coordinate system. The drilling direction was normal to the plane of the workpiece, i.e. the negative Z direction into the workpiece. The friction drilling forces were collected utilizing the LabVIEW SignalExpress data acquisition system. The voltage signal is collected and recorded continuously with the selected sampling rate of 1000 Hz. The related calibration equation was applied to convert voltage to force in Newton.

Based on the recommendation of the friction drilling tool provider, Flowdrill©, the parameters are shown in Table 2. For the drill bit diameter of 5.3 mm, the recommended tool spindle speed is between 1800 rpm and 3300 rpm. For the drill bit diameter of 7.3 mm, the value is between 1500 rpm and 3200 rpm. The recommendation notes that according to different material properties and workpiece thicknesses, the recommended data may be adjusted. For aluminum and non-ferrous materials, the spindle speed of the friction drill bit could be 50 percent higher rpm. Therefore, the ranges from 1800 rpm to 4950 rpm and from 1500 rpm to 4800 rpm are appropriate for

the tool diameter of 5.3 mm and 7.3 mm, respectively. Also, based on the capability of the Bridgeport CNC milling machine, the range between 2000 rpm and 4000 rpm is selected to carry out the friction drilling experiments in the study.

Table 2: Parameters table for Flowdrill© friction drill bit [8]

Thread size	Tool diameter (mm)	Spindle speed (rpm)			Power (kW)	Cycle time (s)
		Minimum	Optimal	Maximum		
M4	3.7	2200	2600	5500	0.7	2
M5	4.5	2000	2500	4800	0.8	2
M6	5.3	1800	2400	3300	1.0	2
M8	7.3	1500	2200	3200	1.3	2
M10	9.2	1200	2000	2800	1.5	3
M12	10.9	1000	1800	2200	1.7	3

Table 3 shows the experiment run matrix. Twelve runs of experiment, labeled as 1-12 are carried out to study the effect of different parameters. The experiments 1-9 are designed to study the effect of spindle speeds, feed rates, and the interaction of the two parameters. For 10-12, different thicknesses of the workpiece (1.25 mm and 2.29 mm), and different friction drill bit diameters (5.3 mm and 7.3 mm) are studied. The

experiments conducted with a variety of combination of input parameters are described in Table 3.

Table 3: Experiment of friction drilling process.

Experiment/run	Workpiece thickness (mm)	Drill bit diameter (mm)	Spindle speed (rpm)	Feed rate (cm/min) (in/min)
1	1.25	5.3	2000	3.81 (1.5)
2	1.25	5.3	2000	6.35 (2.5)
3	1.25	5.3	2000	8.89 (3.5)
4	1.25	5.3	3000	3.81 (1.5)
5	1.25	5.3	3000	6.35 (2.5)
6	1.25	5.3	3000	8.89 (3.5)
7	1.25	5.3	4000	3.81 (1.5)
8	1.25	5.3	4000	6.35 (2.5)
9	1.25	5.3	4000	8.89 (3.5)
10	1.25	5.3	4000	6.35 (2.5)
11	2.287	5.3	4000	6.35 (2.5)
12	2.287	7.3	4000	6.35 (2.5)

4.2 Repeatability test

In order to have good consistency and stability for the entire friction drilling process, the experiment with the exactly same parameters was executed repeatedly. The repeatability of the results is necessary for the reliability of the experiment.

The experiment carries out at 3000 rpm spindle speed with 6.35 cm/min constant feed rate using the thickness of 1.25 mm aluminum alloy workpiece. The chart shows three repeated runs in the same setting and condition. Due to the constant feed rate, the X-axis can be viewed as either time from contact or tool travel from contact. The Y-axis represents the axial thrust force which is the interaction between workpiece and friction drill bit while machining in z direction. The output from the data acquisition was converted to the unit of force, Newton.

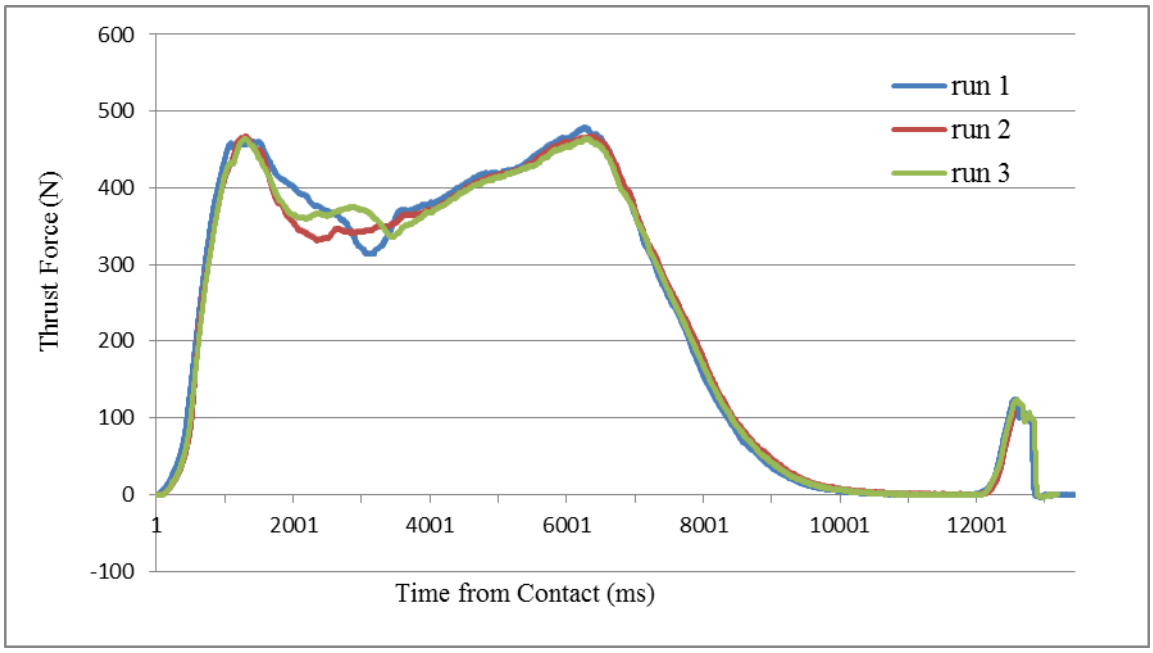

Figure 10: Repeatability test in aluminum alloy friction drilling process.

Figure 10 demonstrates good repeatability in different experiments with the same condition. The three results of the thrust force at the first peak are consistent, so as the second peak. Some inconsistent forces between the first peak and secondary peak where the center points penetrate the material were observed. The amount of lubricant applied and the adhesion of the aluminum to the drill bit may cause the difference in the results. The final peak where the back-extruded material contacts the tool shoulder is also consistent in three experimental results.

4.3 Explanation of the curve of thrust forces

Two significantly different types of the thrust force curves are discovered in the friction drilling experiments. One type of the curve which is consistent with the previous result in the literature review involves two peaks, while another type of the curve is found to contain three peaks. A series of friction drilling tests are executed to study the cause of the difference. For each friction drilling test, while the friction drilling tool travels to a selected position and retracts to the initial position, the thrust force data are recorded.

A series of measured data of the thrust forces in friction drilling of 2.29 mm (0.09 inch) thick aluminum alloy workpiece are shown below in Table 4. The experiments were conducted at 3000 rpm spindle speed with 6.35 cm/min constant feed rate using the Long Flat 5.3 Flowdrill© tungsten carbide drill bit.

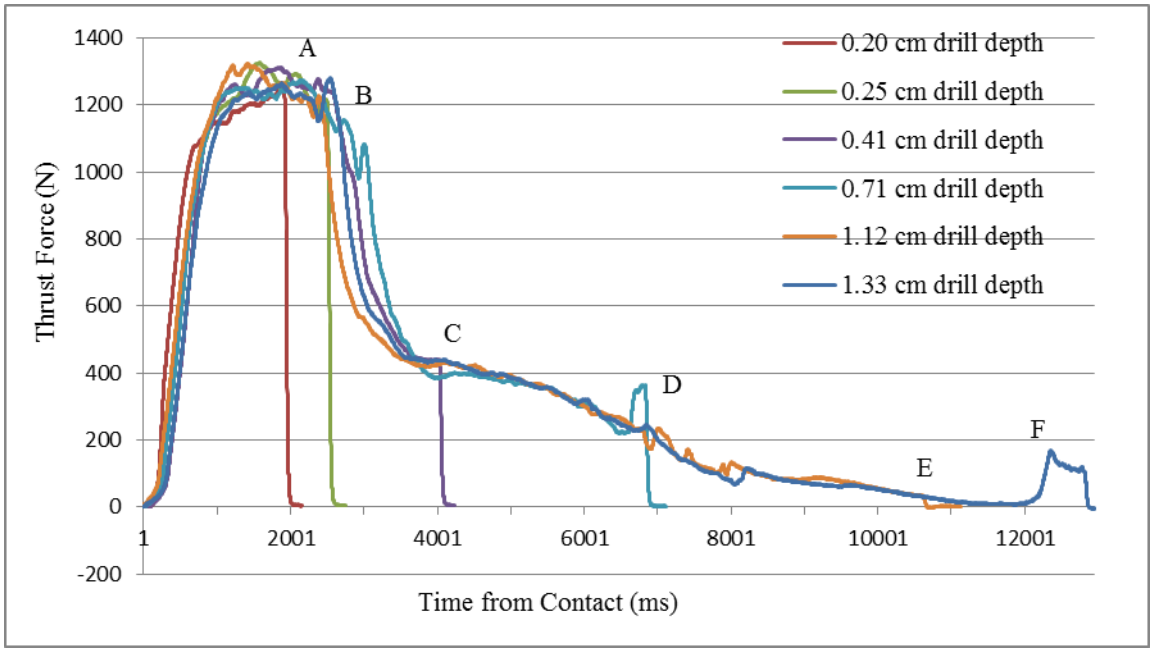

Figure 11: Thrust force curve in 2.29 mm thick aluminum alloy workpiece friction drilling with 3000 rpm spindle speed and 6.35 cm/min feed rate using 5.3 mm drill bit.

Table 4: Thrust force values at various stages for 2.29 mm thick workpiece.

Position	Time from contact (s)	Distance from contact (cm) (inch)	Thrust force (N)
A	2	0.2032 (0.08)	1250
B	2.5	0.254 (0.10)	1152
C	4	0.406 (0.16)	433
D	7	0.711 (0.28)	237
E	11	1.118 (0.44)	33
F	13	1.334 (0.525)	123

(a) Tool travel 0.08 inch from contact at position A.

(b) Tool travel 0.1 inch from contact at position B.

Figure 12: The deformation photomicrographs captured in every separate friction drilling test using 2.29 mm thick aluminum alloy workpiece with 5.3 mm diameter drill bit.

(c) Tool travel 0.16 inch from contact at position C.

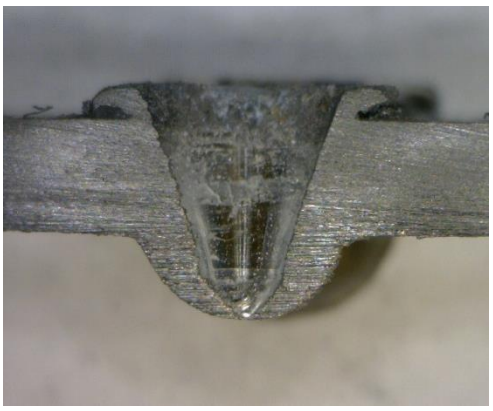

(d) Cross-sectioned view at position C.

Figure 12: Continued.

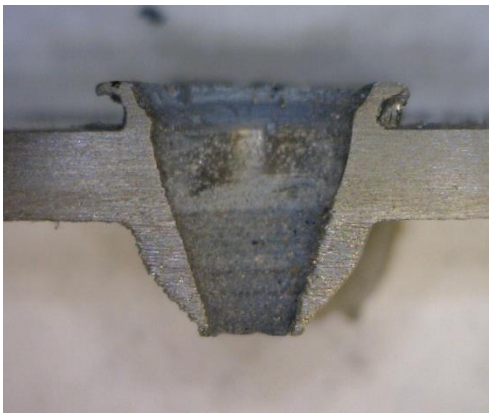

(e) Tool travel 0.28 inch from contact at position D.

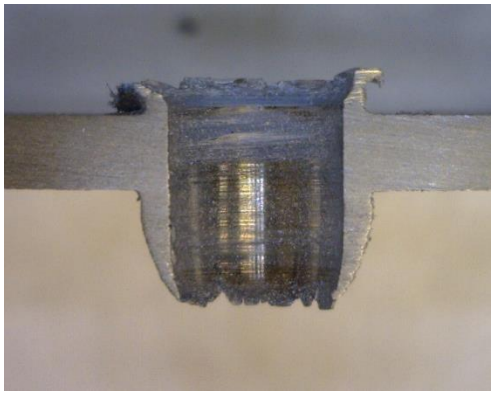

(f) Tool travel 0.44 inch from contact at position E.

Figure 12: Continued.

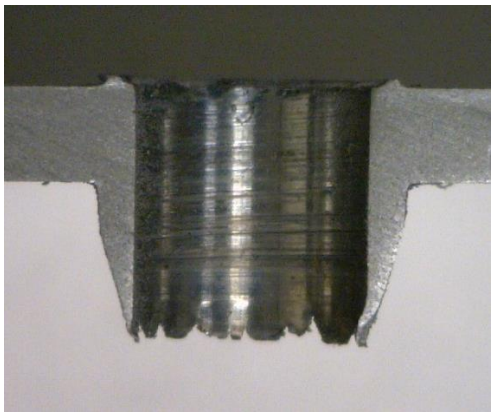

(g) Tool travel 0.525 inch from contact at position F.

Figure 12: Continued.

In Figure 11, the axial thrust force curve in friction drilling 2.29 mm (0.09 inch) thick aluminum alloy 6061-T651 is shown. The first peak that occurs at 0.08 inch of tool travel from contact shows a thrust force of 1250 N. The maximum thrust force position is labeled as A to make an advanced cross-section observation. At position A in Figure 12, the workpiece is slightly dented by the high angle of the center tip. Similar to the conventional twist drilling, the center tool tip plays a critical role in the mechanical indentation of the workpiece [29]. Its high angle and reduced height allow the larger axial forces and more heat in the beginning of the friction drilling. Moreover, the center part spots hole center precisely to prevent wandering at the start of friction drilling. After the first peak, the thrust force decreases rapidly between position B and C. At position B, the distance of tool travel from contact is 0.10 inch. Although the tool travel distance is larger than the workpiece thickness, 0.09 inch, the deflection and ductility of the work

material cause workpiece to deform without fracture. A critical separate friction drilling test is executed at position C of distance of 0.16 inch from contact. The thrust force drops to 433 N which is approximately one-third of the peak value at position C. At this point, the work material is on the verge of fracture. A tiny penetrated hole formed by the tip of the tool center is observed. It indicates that the center part of the friction drill bit contributes a large amount of the thrust force to penetrate the workpiece. After the penetration, the thrust force keeps decreasing in a smaller rate. The conical part starts to rub against the work material to generate more friction heat and soften the material. At position D, the thrust force drops to 237 N. The hole region has been gradually pushed radially and expanded by the conical part. Therefore, smaller thrust force is required to move the friction drill bit downward, since the temperature is high enough to soften the work material. At position E, the cylindrical part configures the complete hole diameter and form the bushing shape. The thrust force at position E is even lower as 33 N. Finally, as the tool travels further downward, the thrust force suddenly uplifts to 123 N which represents the process of trimming the back-extruded work material, so-called boss. At position F, the small peak of thrust force is created by in interaction between the shoulder of the friction drill bit and the boss.

The second type of the thrust force curves while friction drilling 1.25 mm thick aluminum alloy workpiece is shown below in Table 5. The experiment was conducted at 4000 rpm spindle speed with 3.81 cm/min constant feed rate using the Long Flat 5.3 Flowdrill© tungsten carbide drill bit.

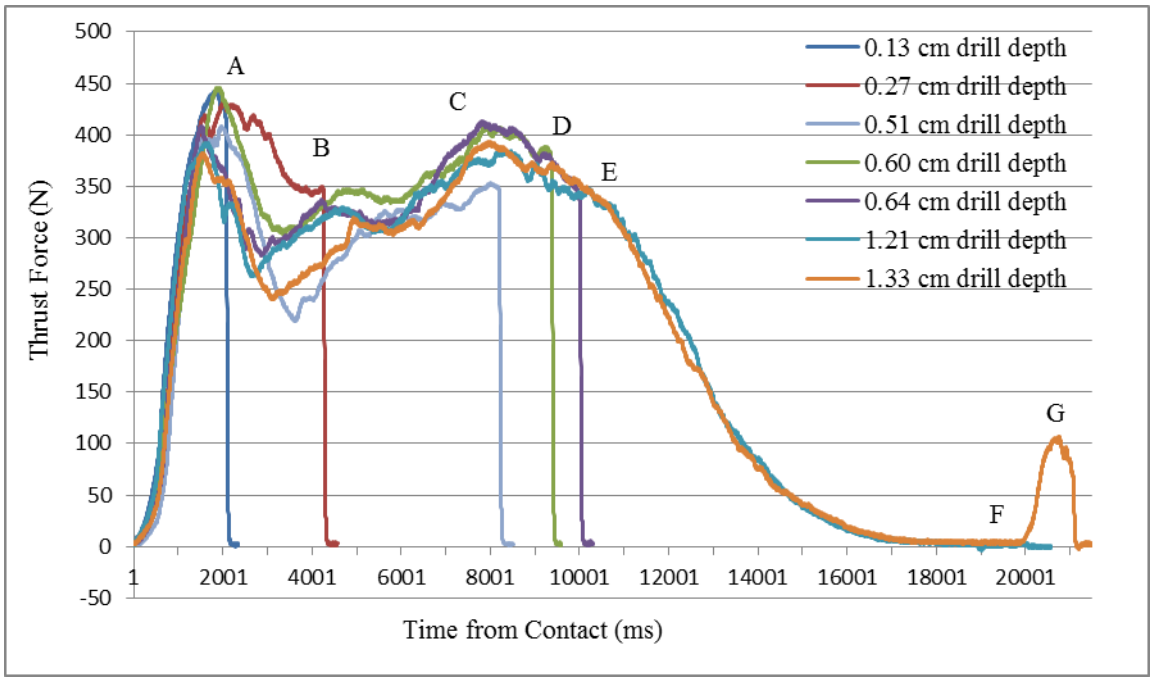

Figure 13: Thrust force curve in 1.25 mm thick aluminum alloy workpiece friction drilling with 4000 rpm spindle speed and 3.81 cm/min feed rate using 5.3 mm drill bit.

Table 5: Thrust force values in every stage for 1.25 mm thick workpiece.

Position	Time from contact (s)	Distance from contact (cm) (inch)	Thrust force (N)
A	2.1	0.127 (0.05)	432
B	4.3	0.267 (0.105)	335
C	8.2	0.508 (0.200)	387
D	9.3	0.597 (0.235)	378
E	10	0.635 (0.25)	354
F	20	1.2065 (0.475)	4.5
G	21	1.3335 (0.525)	92

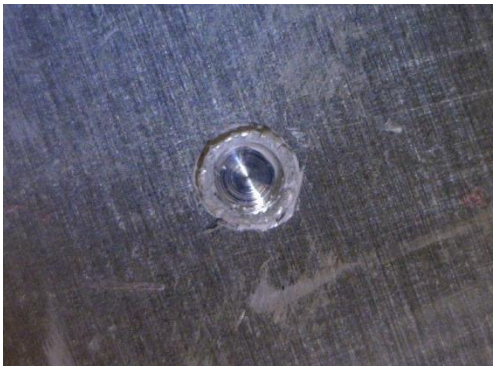

(a) Tool travel 0.05 inch from contact at position A.

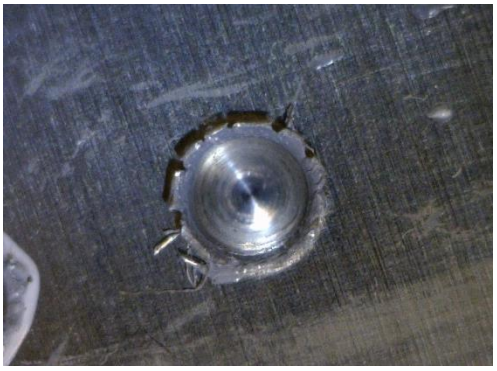

(b) Tool travel 0.105 inch from contact at position B.

Figure 14: The deformation photomicrographs captured in every separate friction drilling test using 1.25 mm thick aluminum alloy workpiece with 5.3 mm diameter drill bit.

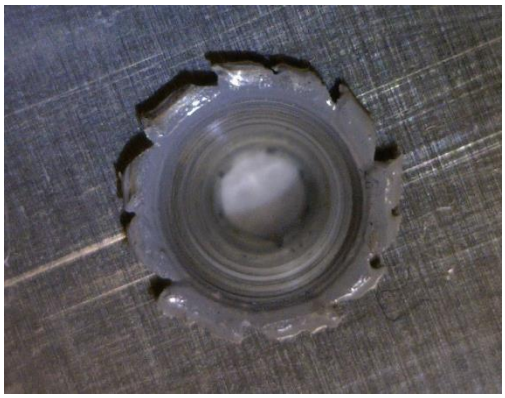

(c) Tool travel 0.2 inch from contact at position C.

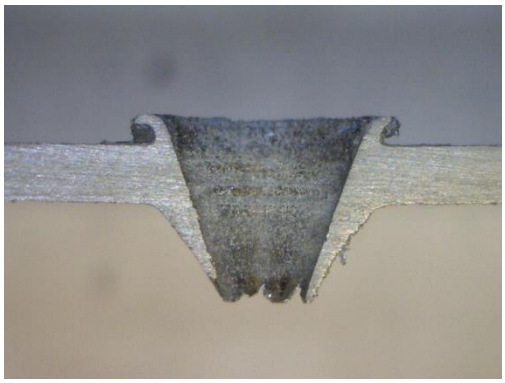

(d) Cross-sectioned view at position C.

Figure 14: Continued.

(e) Tool travel 0.235 inch from contact at position D.

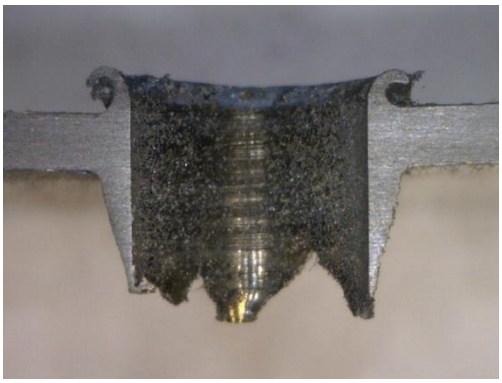

(f) Tool travel 0.475 inch from contact at position F.

Figure 14: Continued.

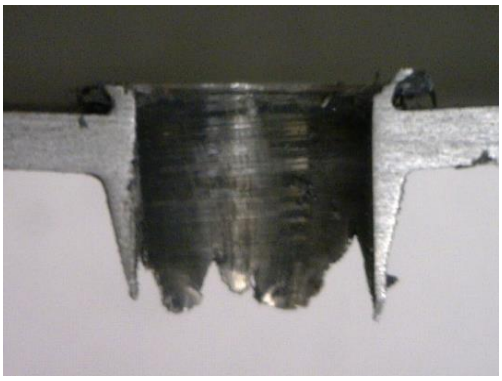

(g) Tool travel 0.525 inch from contact at position G.

Figure 14: Continued.

In Figure 13, the axial thrust force curve in friction drilling 1.25 mm (0.05 inch) thick aluminum alloy 6061-T651 is shown, and the cross sectioned specimen in Figure 14 is shown. The thrust force increases initially. At position A in Figure 14, the first thrust force peak is reached at 432 N as the tool travels 0.05 inch from contact surface. As the tool keeps rotating at 4000 rpm, the temperature in the work region rises due to the frictional heat. The shear stress at the work material reduces as the temperature increases, and therefore the friction coefficient between the drill bit and the workpiece decreases [1]. In other words, the temperature increase causes the work material to soften, and thus the thrust force decreases. At position B, the thrust force drops to 335 N that is approximately three-fourth of the peak value at position A. At this point, the work material is on the verge of fracture. A tiny penetrated hole formed by the tip of the tool center is observed. As the friction drill bit advances, more conical part contacts the

workpiece. The friction increases, as the contact area between the conical part and the workpiece increases. The thrust force once again uplifts to 387 N at position C, which is viewed as second peak of the curve. The conical part begins to involve in deforming thick burr, therefore, the axial thrust force increases to maximum value at C. The thrust force then progressively declines at position D and E, as the cylindrical part begins to deform thinner burr and expand the inner hole diameter. After the hole is completely penetrated, the shoulder part contacts the boss to remove it indicated as the third peak of the thrust force at position G. The thrust force then decreases rapidly to zero as the drill bit retrieves.

4.4 Parameters affecting the thrust force

After completing the interpretation and the repeatability test of the thrust force curve, the study of input parameters with respect to the thrust forces is executed. Different input parameters (spindle speed, feed rate), tool parameters (diameter of the drill bit), workpiece parameters (thickness of the sheet metal) influencing the thrust forces and the geometries of the bushing shape is discussed. The measured thrust force is analyzed to identify the effect of each parameter. The vertical axis represents the axial thrust force interacting between the friction drill bit and the workpiece in the unit of Newton. The horizontal axis represents the time from contact between the friction drill bit and the workpiece, or the distance of drill bit travel when the feed rate maintains constant. The time for the whole friction drilling process depends on the tool feed rate. Although the repeatability test has verified the consistency of the friction drilling process,

every single curve is created by the average of three valid repeated runs. The parametric study is presented in the following sections.

4.4.1 Effect of spindle speed

The experiment for run 1 to run 9 was designed to determine the effect that the rotational speed of the drill bit has on the axial thrust forces as well as the geometries of the bushing shape. The 1.25 mm thickness aluminum alloy sheet metals were used as the work material. The experiments are conducted in 5.3 mm diameter friction drill bit with drill paste on the surface of the tool.

The three following figures present the experimental data of axial thrust forces acquired from three different feed rates, 3.81 cm/min, 6.35 cm/min, 8.89 cm/min, respectively.

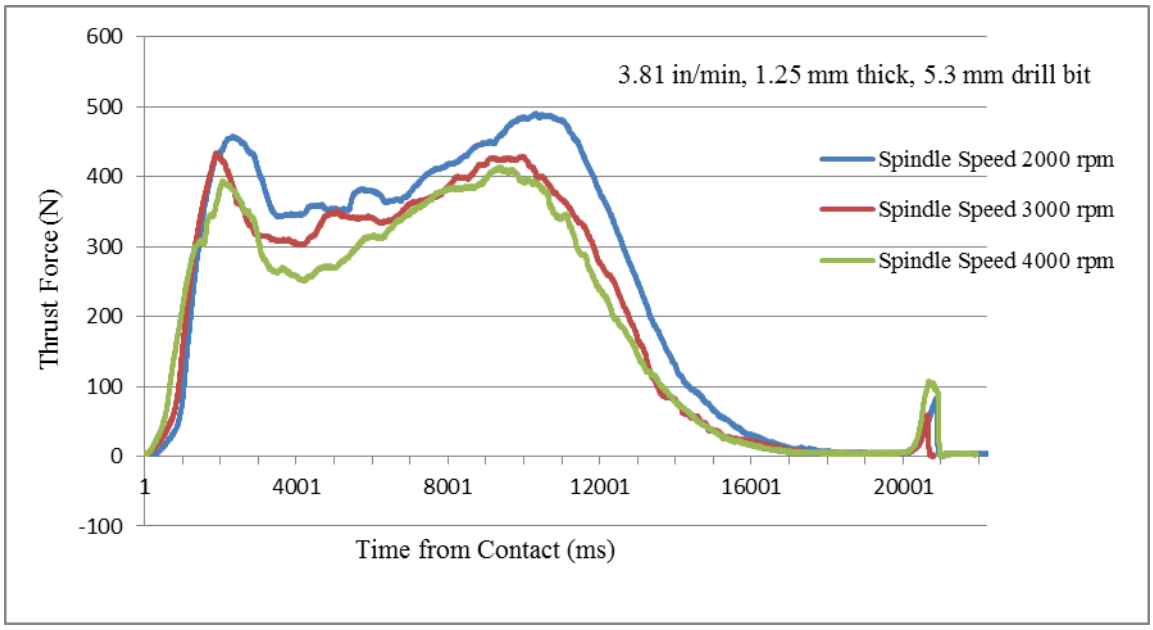

Figure 15: Comparison of the thrust forces with 3.81 cm/min feed rate.

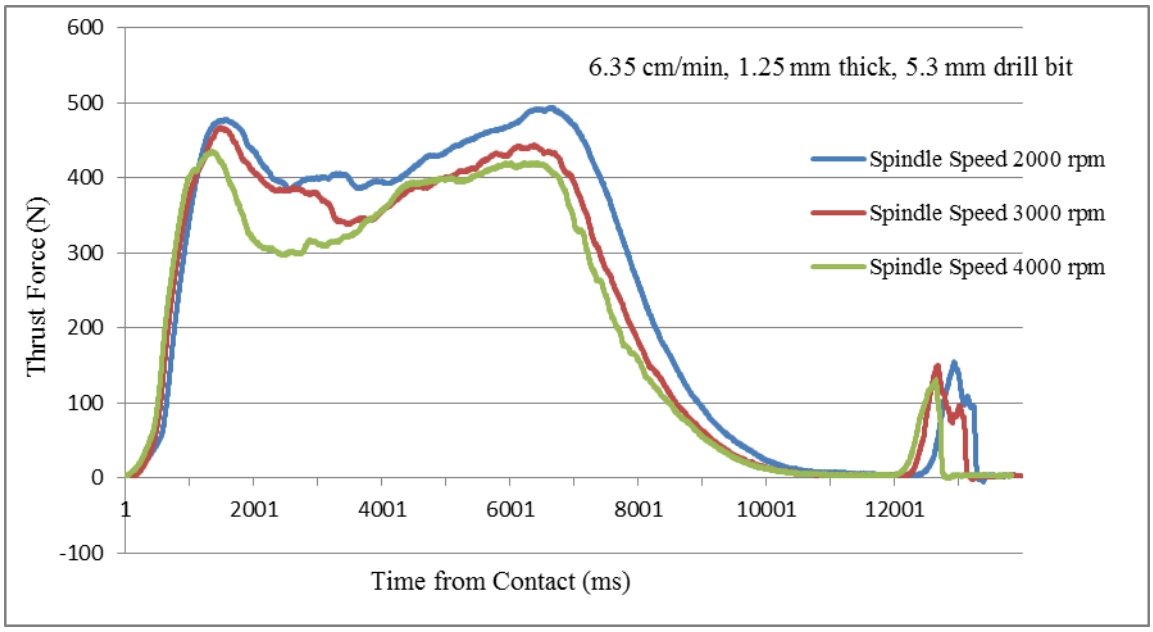

Figure 16: Comparison of the thrust forces with 6.35 cm/min feed rate.

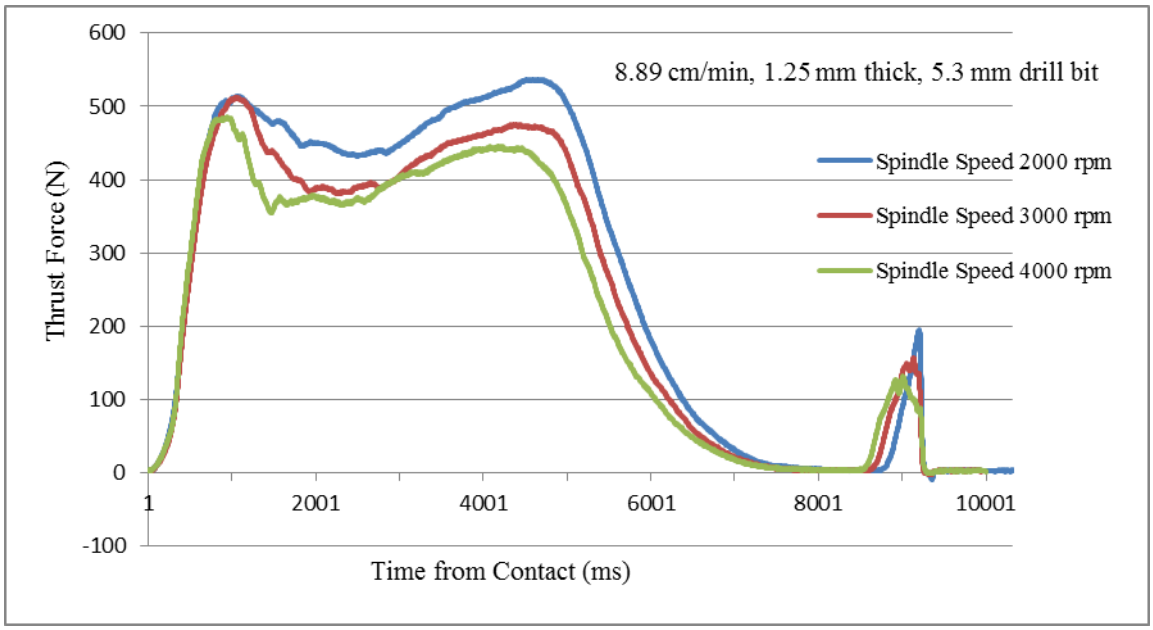

Figure 17: Comparison of the thrust forces with 8.89 cm/min feed rate.

It can be observed that the thrust force is less in friction drilling process while the spindle speed increases. At constant feed rate, higher spindle speed provides more rotations of the tool in unit travel distance as well as unit time, resulting in more frictional heat between the tool and the workpiece. As the temperature rises, the shear stress at the work material reduces, and therefore the friction coefficient between the drill bit and the workpiece decreases [1]. In other words, the increase of the temperature makes the work material soften, and thus the thrust force decreases.

The thrust force measured from the same feed rate increases at the same rate to the first peak. The first peak values vary depending on the spindle speed. At 2000, 3000, and 4000 rpm tool spindle speeds, the peak values are 378, 437, and 448 N for 3.81

cm/min; 426, 450, and 475 N for 6.35 cm/min feed rate; 480, 496, and 507 N for 8.89 cm/min feed rate, respectively. With the same feed rate, the first peak value decreases as the spindle speed increases.

The secondary thrust force peaks are also found decreasing as the spindle speed increases within the same feed rate. The benefit of high tool spindle speed to lower the thrust forces is identified.

4.4.2 Effect of feed rate

The experiment for run 1 to run 9 was also designed to determine the effect of feed rate on the axial thrust forces as well as the geometries of the bushing shape. The 1.25 mm thickness aluminum alloy sheet metals are used. The experiments are conducted in 5.3 mm diameter friction drill bit with drill paste on the surface of the tool.

The three following figures, Figure 18, Figure 19, and Figure 20, present the measured axial thrust forces obtained from three different spindle speeds, 2000, 3000, and 4000 rpm, respectively.

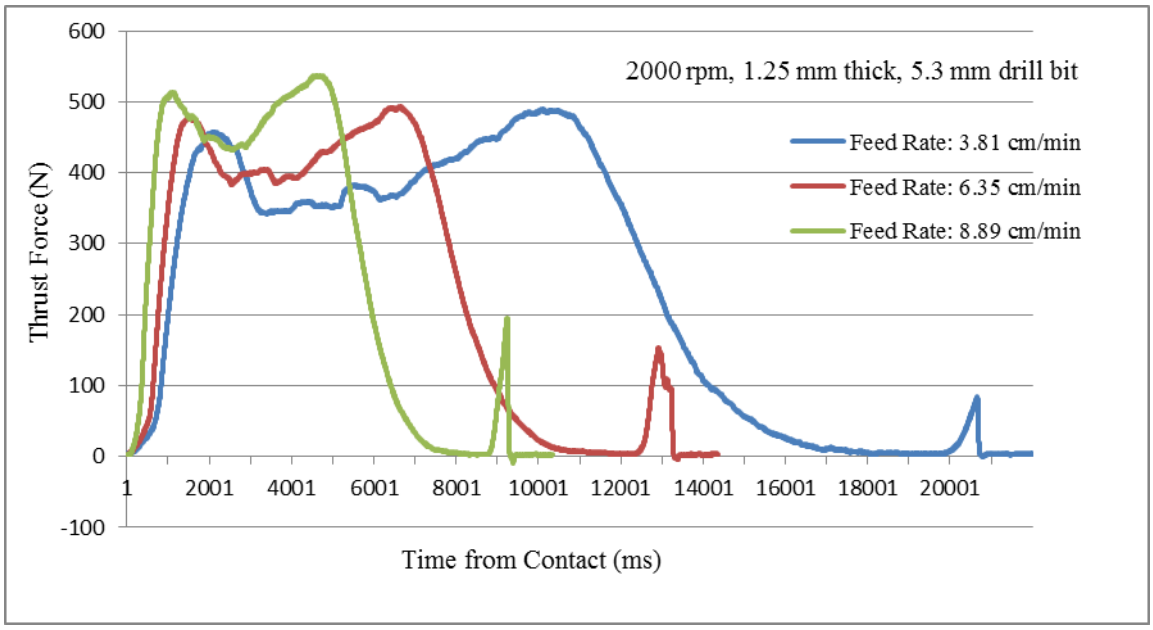

Figure 18: Comparison of the thrust forces with 2,000 rpm spindle speed.

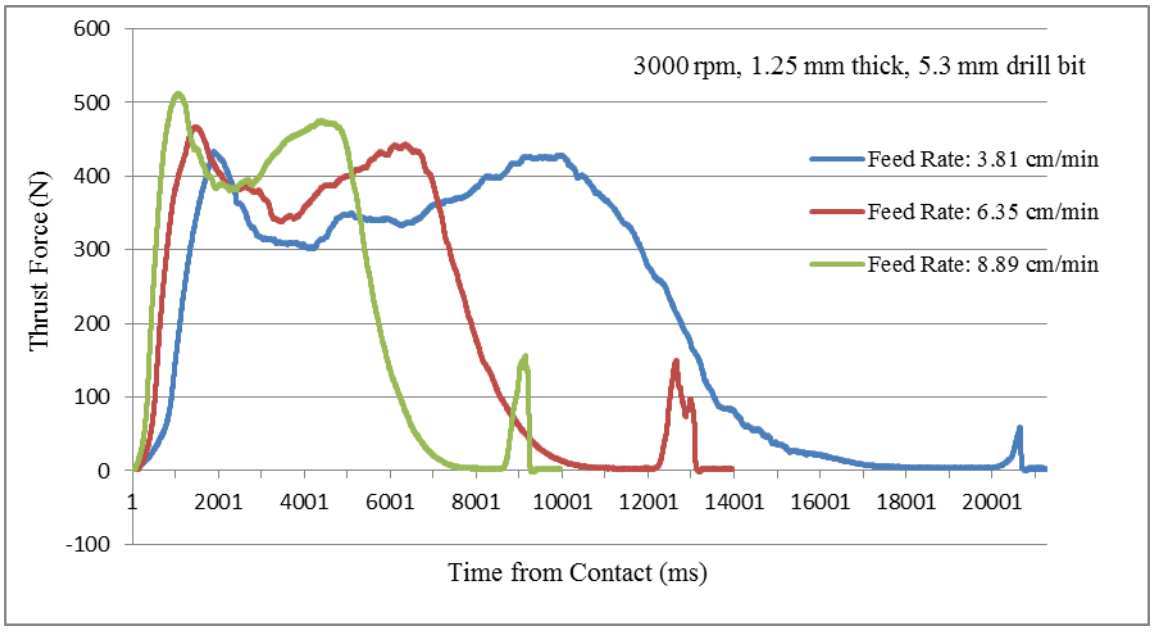

Figure 19: Comparison of the thrust forces with 3,000 rpm spindle speed.

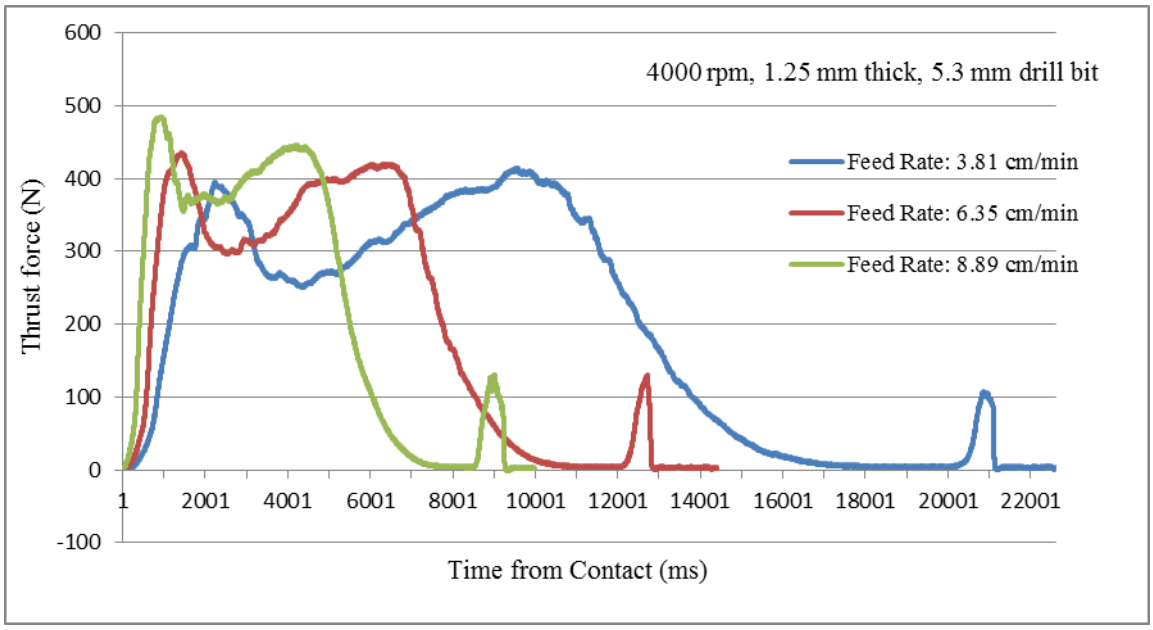

Figure 20: Comparison of the thrust forces with 4,000 rpm spindle speed.

According to the plots, the thrust force increases at a higher rate to the peak in higher feed rate, 3.5 inch per minute, which means shorter time is taken to reach the first thrust force peak in higher feed rate. The cycle time is reduced in the friction drilling process with higher feed rate. For the 3.81, 6.35, and 8.89 cm/min feed rate, the time to generate a hole is 21, 13, and 9 seconds for 2000, 3000, and 4000 rpm spindle speed, consistently due to the constant feed rates. However, the first, second, and third thrust force peak values increase, as the feed rate increases. At 3.81, 6.35, and 8.89 cm/min feed rate, the maximum peak values are 483, 490, and 530 N for 2000 rpm spindle speed ; 431, 463, and 508 N for 3000 rpm spindle speed ; 404, 446, and 470 N for 4000 rpm spindle speed, respectively. The contact process period shortened at higher feed rate

indicates lower drilling temperature gained. Lower temperature results in the requirement of larger axial thrust force to drill a hole due to the increase of the shear stress at the work material.

4.4.3 Effect of workpiece thickness

To determine the effect that the thickness of the workpieces has on the axial thrust forces as well as the geometries of the bushing shape, the experiment for run 10 to run 12 was designed. The 1.25 mm and 2.29 mm thickness aluminum alloy sheet metals are used. The input parameters of 3000 rpm spindle speed and 6.35 cm/min feed rate are selected. Different diameters, 5.3 mm and 7.3 mm, of the friction drilling bit with drill paste are adopted as a comparison.

The following figures introduce the experimental data of axial thrust forces acquired from different thickness of the workpieces.

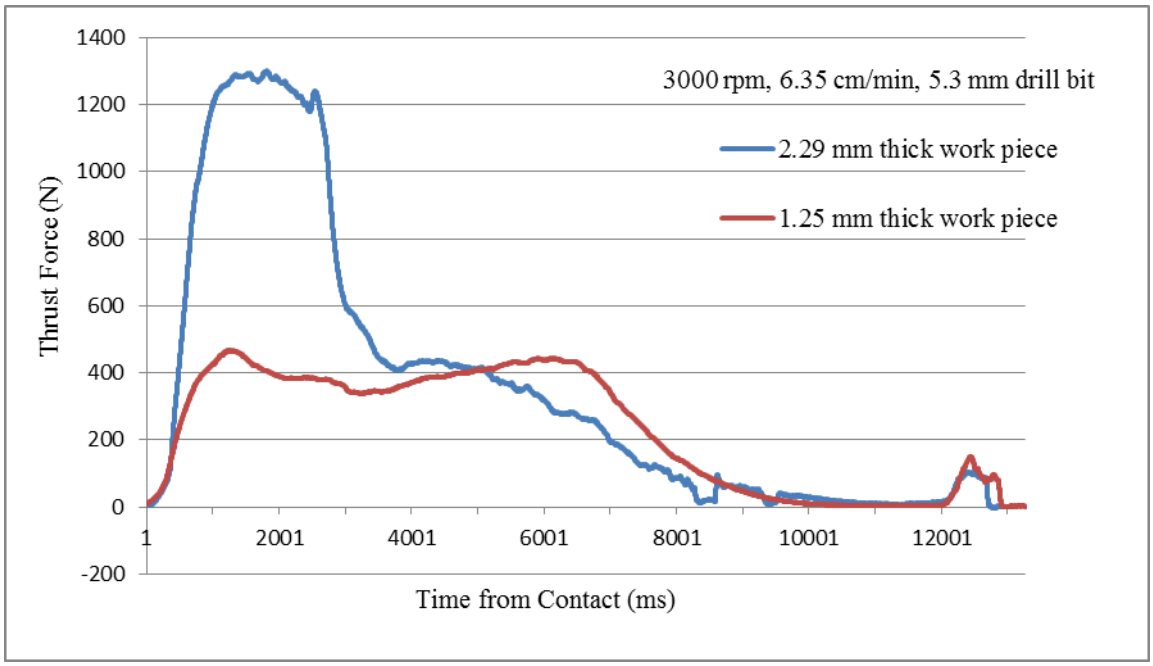

Figure 21: Comparison of the thrust forces for different workpiece thicknesses using 5.3 mm friction drill bit.

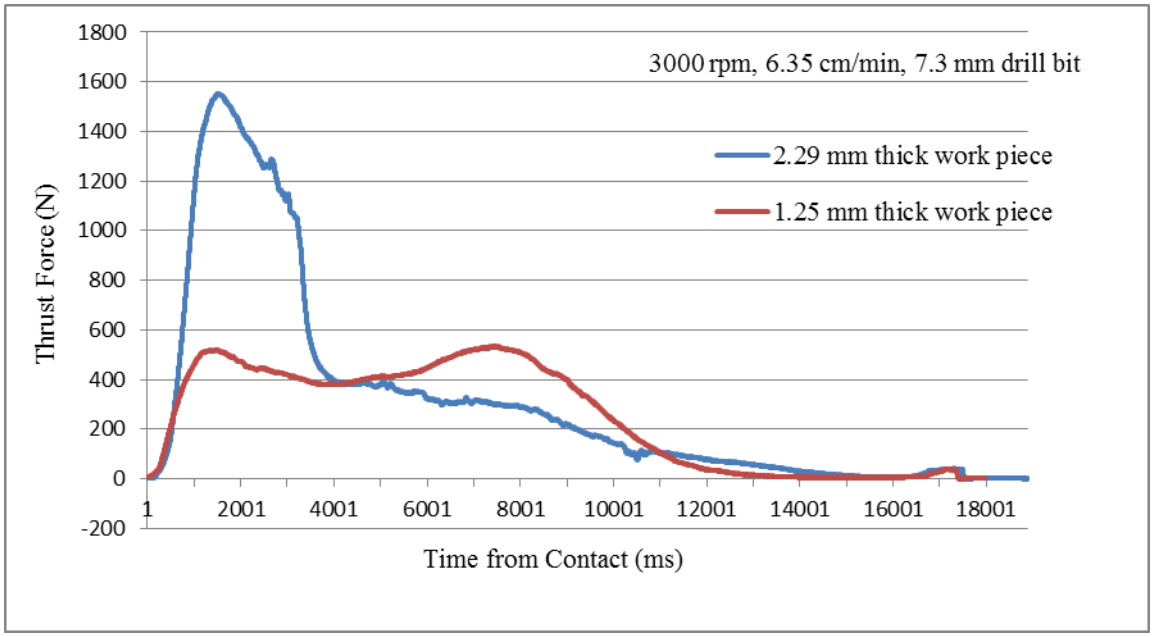

Figure 22: Comparison of the thrust forces for different workpiece thicknesses using 7.3 mm friction drill bit.

It is obvious that a much higher thrust force is required for friction drilling the 2.29 mm thick workpiece compared to the 1.25 mm thick workpiece. The increase of the thrust forces is noticed when the workpiece thickness increases, since the larger material volume is to be deformed. For 2.29 mm thick workpiece, a larger amount of material needs to be deformed before the workpiece was penetrated. With 5.3 mm diameter friction drill bit, 1276 and 451 N thrust forces are required to penetrate the work material for 2.29 and 1.25 mm thick workpiece, respectively. Therefore, it indicates that the larger thrust force is required to complete a friction drilled hole in thicker workpiece.

4.4.4 Effect of tool diameter

To determine the effect of the tool diameter on the axial thrust forces as well as the geometries of the bushing shape, the experiments for run 10 to run 12 are conducted. The Long Flat 5.3 Flowdrill© and the Long Flat 7.3 Flowdrill© tungsten carbide drill bit are used. The input parameters of 3000 rpm spindle speed and 6.35 cm/min feed rate are selected to conduct the experiments. The 1.25 mm and 2.29 mm aluminum alloy workpiece thickness are used for comparison.

The following figures introduce the experimental data of axial thrust forces acquired from different diameters of the friction drill bits.

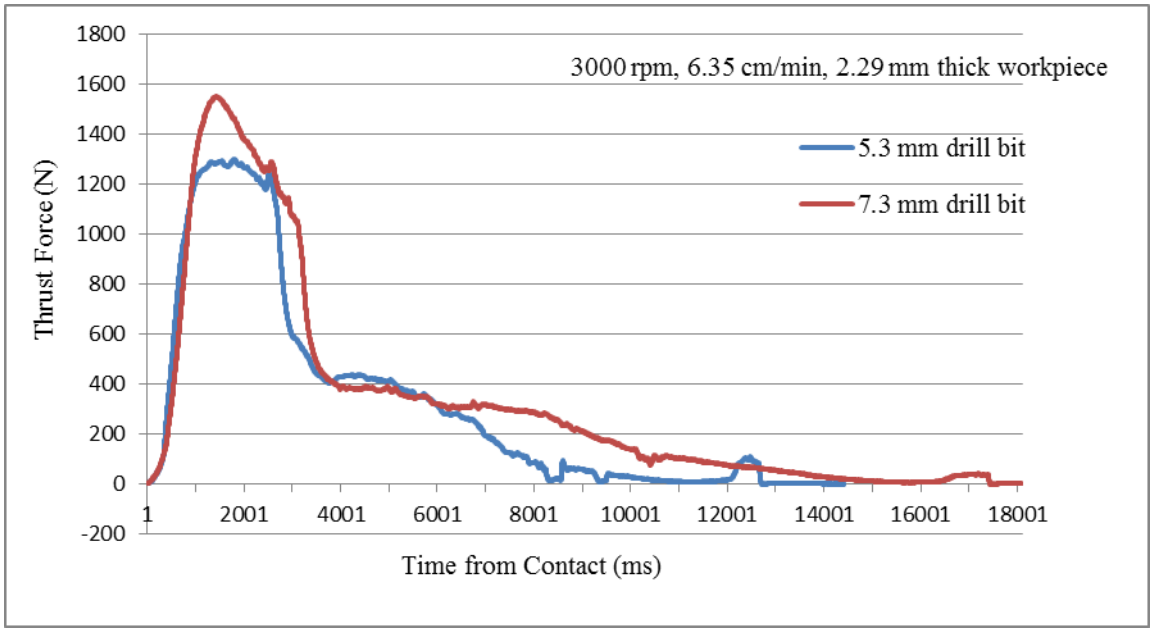

Figure 23: Comparison of the thrust forces for different tool diameters using 2.29 mm thick workpiece.

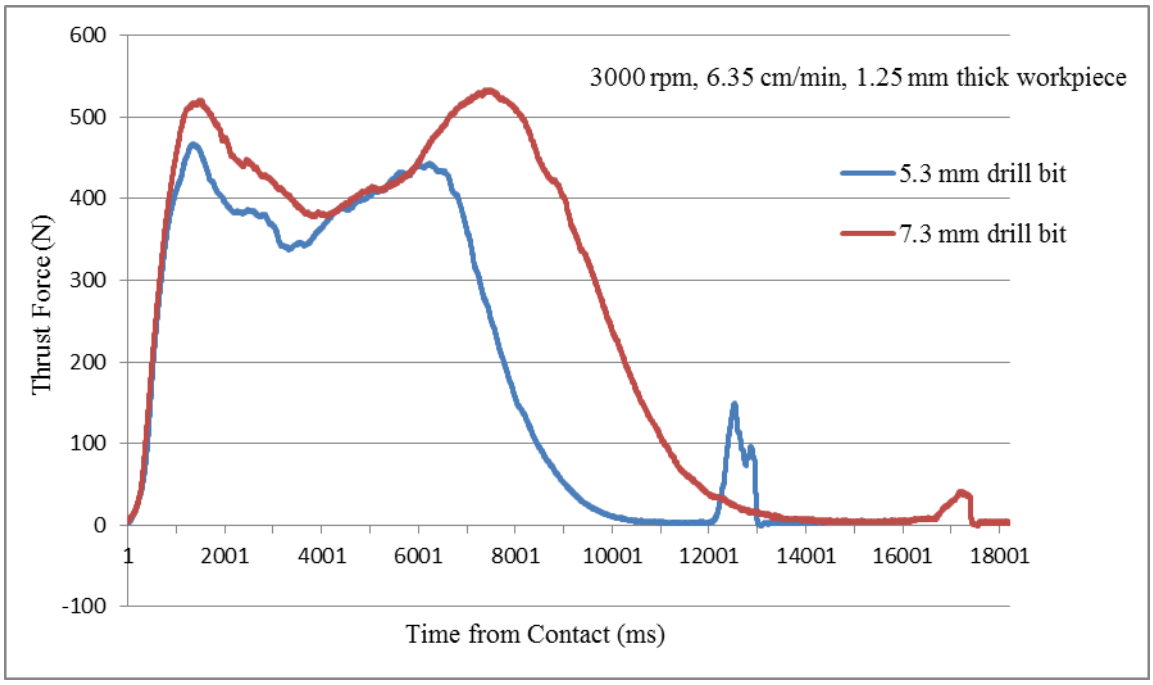

Figure 24: Comparison of the thrust forces for different tool diameters using 1.25 mm thick workpiece.

Higher thrust forces required in the friction drilling process with the larger tool diameter in both cases. A larger amount of material needs to be deformed before the workpiece was penetrated. The increase in deformation volume when a larger drill bit is used reinforces the shear stress at the work material. The tool with larger diameter is also longer. Therefore, at the same feed rate, it takes more time to complete a friction drilling process.

The final peaks in thrust force curve represent the process of trimming the back-extruded work material, the so-called boss. The shoulder of the friction drill bit contacts the boss creates the peak of thrust force. Larger interaction area between the tool and

work material increases the temperature in the work zone including the back-extruded boss. Therefore, less axial thrust force is required to remove the heated material.

4.4.5 Combination effect of spindle speed and feed rate

It has been indicated that the increase of spindle speed and the decrease of feed rate both reduce the required thrust forces. However, within the certain range discussed in the research, the investigation of the combination effect of both factors is required to point out the dominant factor. To determine the combination effect that the spindle speed along with feed rate has on the axial thrust forces, the experiment for run 1 to run 9 was required. The 1.25 mm thick aluminum alloy sheet metal is used in friction drilling by 5.3 mm diameter drilling bit with drill paste.

At 3.81, 6.35, and 8.89 cm/min feed rate, the maximum peak values are 483, 490, and 530 N for 2000 rpm spindle speed ; 431, 463, and 508 N for 3000 rpm spindle speed ; 404, 446, and 470 N for 4000 rpm spindle speed, respectively. Figure 25 introduces the experimental data of axial thrust forces acquired from different input variables.

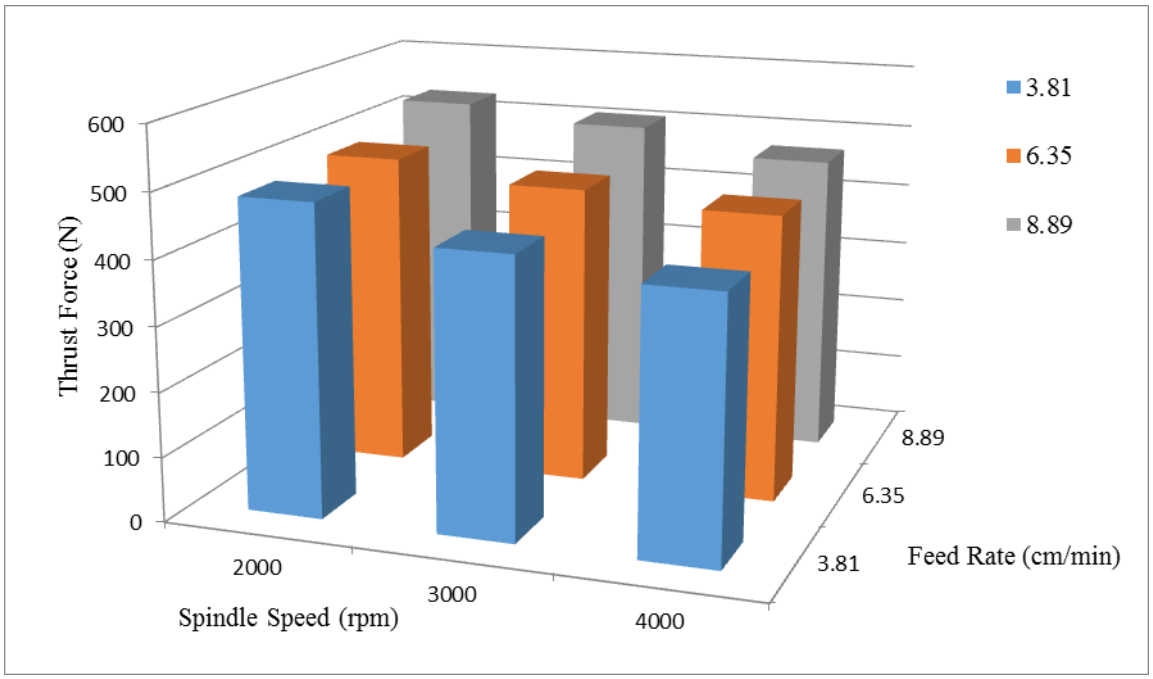

Figure 25: Combination effect of spindle speed and feed rate on the thrust forces in friction drilling 1.25 mm thick workpiece with 5.3 mm drill bit.

Let the 3000 rpm spindle speed with 6.35 cm/min feed rate set as the reference condition. The experimental result indicates that the increase of spindle speed and the decrease of feed rate both reduce the required thrust forces. In accordance with the result, the thrust force reduces by 12.7 percent to 404 N as the spindle speed increases and simultaneously the feed rate decreases; in contrast, the thrust force increases by 14.5 percent to 530 N as the spindle speed decreases and simultaneously the feed rate increases. In the complementary situation, the dominant factor between spindle speed and feed rate is able to emerge. The thrust force enhances by 1.51 percent to 470 N as the spindle speed increases and simultaneously the feed rate increases. However, the

thrust force enhances by 4.32 percent to 483 N as the spindle speed decreases and simultaneously the feed rate increases. It is obvious that within the studied range, the spindle speed has more dominant influence on the thrust force than the feed rate.

4.5 Sample characterization results in friction drilling

The axial thrust force curves generated from combinations of spindle speed, feed rate, workpiece thickness, and drill bit diameter in friction drilling experiments are investigated. Qualitative sample characterization results are shown and discussed in the section. To evaluate the quality of holes in friction drilling, the shape of bushing is an important criterion. The quality of bushing shape is observed and judged via cylindricality, effective length, cracks, and petal formation [9].

The specimens are prepared for microscopy examination. The workpieces with the friction drilled hole are sheared by the cutting blade at the center of the hole. The cross-sectioned edge of the workpiece is manually polished using finer sand papers progressively. The preparation facilitates the optical microscopy examination. Dino-Lite digital microscope is used to capture the cross-sectioned images of the friction drilled workpieces from effective views. The views of the bushing shape from top side of the workpiece and from cross section side of the identical friction drilled hole are presented to compare different features of the bushings.

The figures show low magnification optical images of the cross-sectioned workpieces. The photomicrographs present the cross-sectional view parallel to the polished plane which is feasible to examine the most information of the bushing feature.

The material of the polished specimens is 1.25 mm thick aluminum alloy sheet metal. The effect of drilling variables on the shape of bushing and the hole geometries is discussed. The selected drilling parameters are 2000, 3000, and 4000 rpm spindle speed with 3.81, 6.35, and 8.89 cm/min feed rate conducted using a 5.3 mm diameter friction drill bit with drill paste on the surface of the tool. Some distinct geometries such as length of bushing, cracking, petal formation, and denting of the workpieces between different drilling parameter are able to be observed in the photomicrographs.

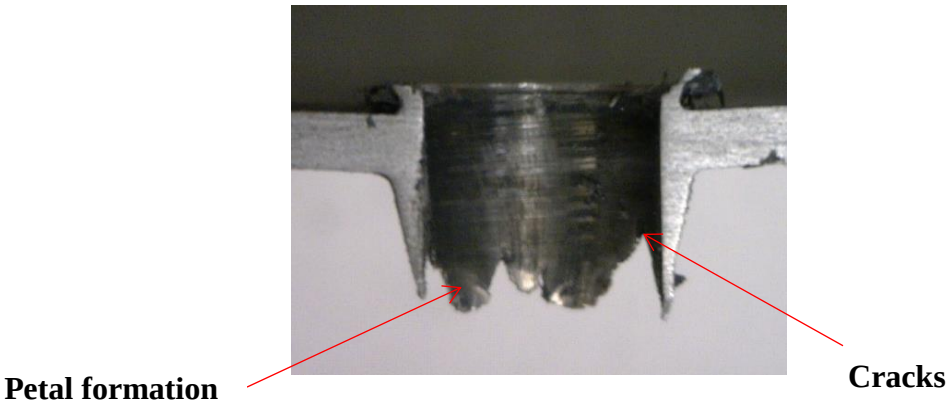

(a) 3.81 cm/min feed rate

Figure 26: Bushing cross section formed by friction drilling 1.25 mm thick aluminum alloy at 4000 rpm with 5.3 mm diameter drill bit (a) 3.81 cm/min (b) 6.35 cm/min (c) 8.89 cm/min.

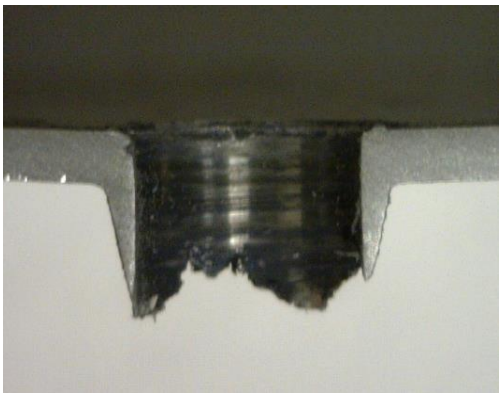

(b) 6.35 cm/min feed rate

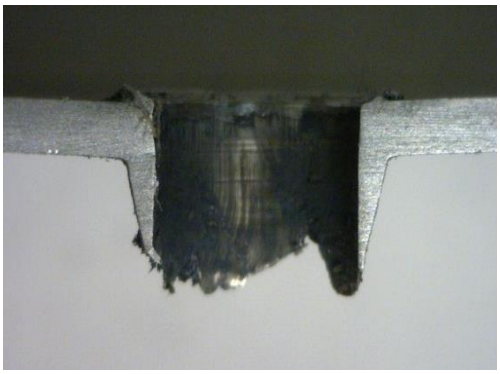

(c) 8.89 cm/min feed rate

Figure 26: Continued.

Figure 26 shows bushing cross section in friciton drilling 1.25 mm thick aluminum alloy workpieces at 4000 rpm spindle speed with different feed rates. The tool feed rates are 3.81 cm/min, 6.35 cm/min, and 8.89 cm/min in Figu (a)-(c), respectively. The cross-sectioned view is capable of revealing different features of the friction drilled hole area clearly. The cracking and petal formation are undesirable bushing features in

friciton drilling sheet metals. For further application, these undesirable characteristics influence the effective length and strength for threading. In other words, the cracking and petal formation destroy the useful surface area to limit the loading capability of threaded holes.

The bushing geometry is slightly improved by the decrease of the feed rate. As the feed rate decreases, the length of bushing extends. However, compared to the effect of spindle speed, the effect of feed rate on the bushing is relatively small. The raised feed rate promotes more rapid deformation of the work material in lower work zone temperature. The work hardening caused by the rapid deformation reduces the plasticity of the work material. The bushing extrusion length is therefore shortened at high feed rate and low temperature condition.

As the feed rate increases, the bending of the workpiece becomes more apparent. Referred to the thrust force curves in Figure 20, concerning the comparison of different feed rates at constant 4000 rpm spindle speed, the larger thrust forces are required at higher feed rate. The shortened friction drilling period at higher feed rate implies the generation of lower drilling temperature. As a result, the larger axial thrust forces are required to drill a hole at lower temperature due to the increase of the shear stress at the work material. Therefore, under the larger loading of external force perpendicular to the plate, the larger deflection of the sheet metal near the hole is observed.

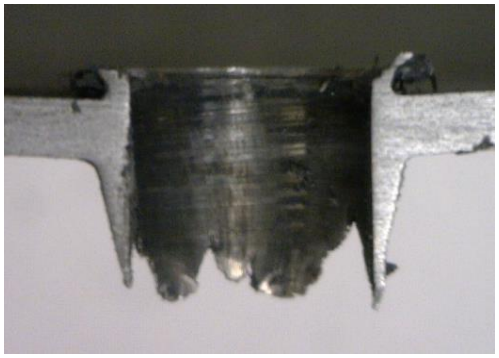

(a) 4000 rpm

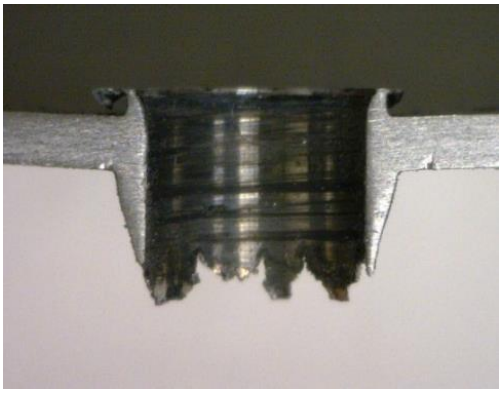

(b) 3000 rpm

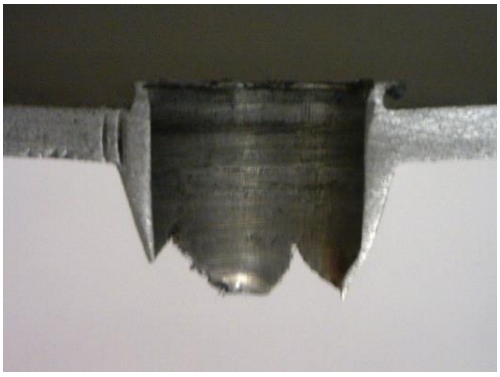

(c) 2000 rpm

Figure 27: Bushing cross section formed by friction drilling 1.25 mm thick aluminum alloy at 3.81 cm/min with 5.3 mm diameter drill bit (a) 4000 rpm (b) 3000 rpm (c) 2000 rpm

Figure 27 shows bushing cross section in friciton drilling 1.25 mm thick aluminum alloy workpieces at 3.81 cm/min feed rate with different spindle speeds. The executed tool spindle speeds are 4000, 3000, and 2000 rpm in Figure 27 (a)-(c), respectively. The 5.3 mm diameter friciton drill bit is carried on with drill paste on the surface of the tool. The cross-sectioned view are capable of revealing different features of the friction drilled hole area clearly.

In the cross-sectioned photomicrographs, the improvement of bushing geometry is observed along the increase of spindle speeds. As the spindle speed increases, the height of bushing extends. Referred to the comparison of spindle speeds at constant 3.81 cm/min feed rate in Figure 15, the thrust force is less in friction drilling process while the spindle speed increases. At constant feed rate, higher spindle speed provides more rotations in unit time, resulting in more frictional heat between the tool and the workpiece. As the temperature rises, the work material becomes more ductile and formable, and therefore the bushing height extends.

The benefit of high spindle speed to lower the thrust forces and bending of the work material is identified. Not only the decrease of feed rates, but also the increase of spindle speeds reduces the bending of the workpiece due to the effect of lower axial thrust forces.

(a) 1.25 mm thick workpiece

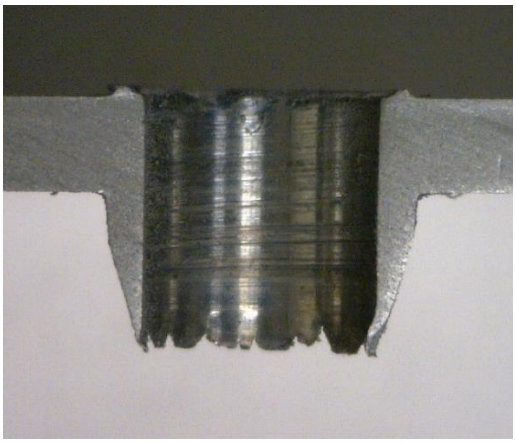

(b) 2.29 mm thick workpiece

Figure 28: Bushing cross section formed by friction drilling (a) 1.25 mm thick and (b) 2.29 mm thick aluminum alloy at 3000 rpm with 3.81 cm/min using 5.3 mm diameter drill bit.

Figure 28 shows bushing cross section in friciton drilling two different thickness aluminum alloy workpieces at 3000 rpm spindle speed with 3.81 cm/min feed rate. The result of the executed workpiece thickness are 1.25 mm and 2.29 mm shown in Figure

28 (a) and (b), respectively. The 5.3 mm diameter friciton drill bit is carried on with drill paste on the surface of the tool. The cross-sectioned view are capable of revealing different features of the friction drilled hole area clearly.

The cracking and petal formation are undesirable bushing features in friciton drilling sheet metals. It can be experimentally observed that more petals are formed in friction drilling the 2.29 mm thick workpiece using the identical 5.3 mm diameter drill bit. In friciton drilling process, t/d ratio is one of the important parameters, where t represents the thickness of the workpiece, and d represents the diameter of the friction drill bit. A large t/d ratio indicates that larger deformed material volume generates the bushing. The t/d ratio is highly related to the petal formation [9]. At a larger t/d ratio between Figure 28 (b) and Figure 28 (a), 0.43 and 0.24 respectively, the bushing cross section shows the better cylindricality, and the petal formation with smaller cracks. With the sufficient work material thickness for a certain hole diameter, the formed bushing suffers less fracture and radial strain that cause ruptures at the hemline [19].

The bending of the workpiece is more apparent in the workpiece thickness of 1.25 mm in Figure 28 (a). Due to larger stiffness of the 2.29 mm thick workpiece, under the same input parameters, the smaller deflection of the sheet metal is observed near the hole.

(a) 5.3 mm diameter drill bit

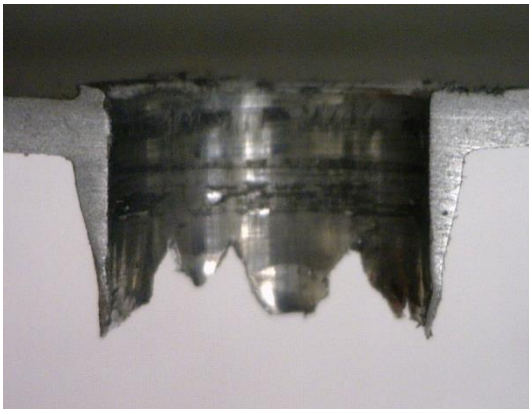

(b) 7.3 mm diameter drill bit

Figure 29: Bushing cross section formed by friction drilling 1.25 mm thick aluminum alloy at 3000 rpm with 3.81 cm/min using (a) 5.3 mm and (b) 7.3 mm diameter drill bit.

Figure 29 shows bushing cross section in friciton drilling 1.25 mm thick aluminum alloy workpieces at 3000 rpm spindle speed with 3.81 cm/min feed rate. The 5.3 mm and 7.3 mm diameter friciton drill bits respectively in Figure 29 (a) and (b) are

carried on with drill paste on the surface of the tool. The cross-sectioned view are capable of revealing different features of the friction drilled hole area clearly.

The cylindricality are desirable bushing features in friciton drilling sheet metals. While friction drilling the 1.25 mm thick workpiece, it is observed that more cylindrical shape is formed using the 5.3 mm diameter drill bit than using 7.3 mm diameter drill bit. At a larger t/d ratio between Figure 29 (a) and Figure 29 (b), 0.24 and 0.17 respectively, the bushing cross section shows the better cylindricality, and the petal formation with smaller cracks. With a certain t/d ratio, the formed bushing suffers less fracture and radial strain that cause ruptures at the hemline [19].

The bending of the workpiece is more apparent in the friciton drilled hole diameter of 7.3 mm in Figure 29 (b). Due to larger external axial loading perpendicularly to the surface of the workpiece, the larger deflection is observed at the 7.3 mm diameter hole zone.

5. IMPROVEMENT OF THE HOLE AND BUSHING SHAPE

5.1 Introduction

In friction drilling, the work material deformed from the friction drilled hole contributes to form boss and bushing. The length of the bushing is about three times thick as the former workpiece [30]. Its additional thickness provides more strength and support to thread the hole. The objective to form bushing on the thin-walled workpiece, sheet metal, or tube is to joint devices more efficiently.

The novel approach with the aim to improve the bushing shape will be introduced. The approach is to carry out the friction drilling experiment with a well-designed lower die which can control the bushing material to a desirable shape in friction drilling process.

Friction drilling experiments with novel approach are conducted in selected input parameters. The axial thrust forces are measured and the geometries of the bushing are studied. The friction drilling forces are collected by utilizing the dynamometer as well as LabVIEW SignalExpress data acquisition system. The voltage signal is recorded continuously with the selected sampling rate of 1000 Hz, and then applied to Voltage-Newton calibration equation. The bushing shape geometries are presented by cross section view. Dino-Lite digital microscope is used to capture the cross-sectioned photomicrographs of the friction drilled workpieces with better magnification and resolution.

5.2 The design of the lower die

The novel fixture is design and manufactured for lower die friction drilling. The end mill is used to cut the 1.2 mm depth shallow slot for placing the work material. Four holes at corners are drilled and threaded to fix the workpiece by bolts and washers. The deep slot to allow for clearance of the drill bit is replaced by the precise holes. The hole contains a 5.3 mm diameter deep hole to accommodate the friction drill bit and 6.35 mm (1/4") diameter step to hold the deformed material. The deformed material is constrained by the upper step cavity to establish a better shape of bushing.

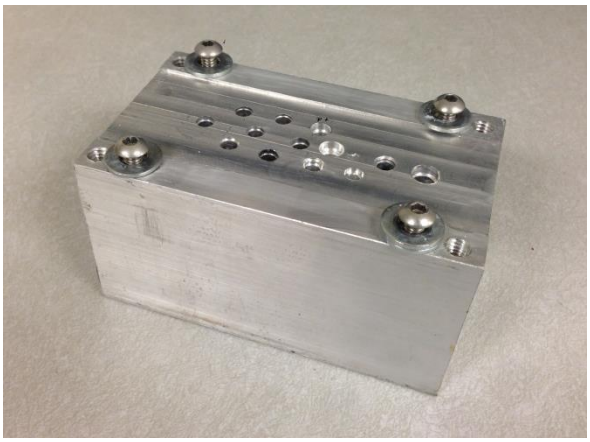

Figure 30: The fixture designed and manufactured for lower die friction drilling.

The geometry of the cavity in the lower die is expected to play an important role in the quality of the bushing shape. The stepped-hole contains three essential parameters, i.e. lower hole diameter d_1, upper hole diameter d_2, and upper hole depth h as shown in

Figure 31. The figure illustrates the cross-sectioned view of the stepped-hole in the lower die.

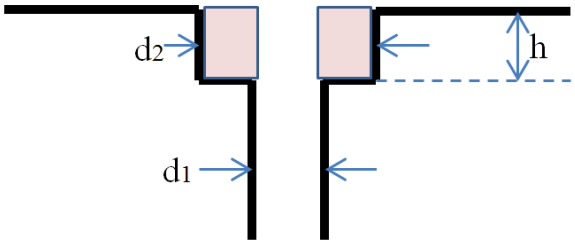

Figure 31: The geometry of stepped-hole in side view of the lower die.

To prevent the damage of the friction drill bit and the CNC machine, calculation is necessary for the design of the stepped hole in the lower die. Some assumptions are made to simplify the calculation of the stepped hole:

a) The deflection of the metal sheet is negligible.

b) No material adhesion from the workpiece to the friction drill bit.

c) The density of work material does not change after a hole is formed.

In the friction drilling process, the softened work material deformed from the friction drilled hole contributes to the forming of boss and bushing, while a large portion

of material goes to bushing. For the 1.25 mm thick workpiece drilled by 5.3 mm diameter friction drill bit, the volume of the deformed material is calculated by

$$V = t * \frac{1}{4}\pi {d_1}^2 \tag{1}$$

$$= 1.25 * \frac{1}{4}\pi * 5.3^2$$

$$= 27.58$$

where V represents the volume of the deformed work material, t represents the thickness of the workpiece, and d_1 represents the diameter of the friction drill bit.

The work material at the drilled hole deforms to make the shape of bushing, and fill into stepped hole in the lower die. The relation between the volume of original work material and the hole with bushing can be described in the following equations.

$$\frac{1}{4}\pi {d_2}^2 h - \frac{1}{4}\pi {d_1}^2 h \geq \frac{1}{4}\pi {d_1}^2 t \tag{2}$$

$$\left({d_2}^2 - {d_1}^2\right) * h \geq {d_1}^2 * t \tag{3}$$

where d_1 represents the diameter of the friction drill bit, also the lower hole diameter, d_2 represents the upper hole diameter, h represents the depth of the step, and t represents the workpiece thickness. Therefore, the design of the stepped-hole in Table 6 in the lower die is based on the relation derived above.

Table 6: The parameters applied in the stepped-hole of the lower die.

design	d_1 (mm)	d_2 (mm)	h (mm)	t (mm)
#1	5.30	6.33	2.60	1.25
#2	5.30	6.37	2.00	1.25

5.3 Lower die friction drilling experiment

In lower die friction drilling, the workpiece is completely supported on the fixture to avoid large deflection during the friction drilling process. The workpiece used is aluminum alloy 6061-T651 with the thickness of 1.25 mm, and clamped by the bolts and washers to stay firmly inside the shallow step. This fixture is mounted on the dynamometer on the CNC milling machine for measuring the forces. The friction drilling forces are collected by LabVIEW SignalExpress data acquisition system. The voltage signal is recorded continuously with the selected sampling rate of 1000 Hz, and then applied to Voltage-Newton calibration equation.

5.3.1 Lower die effect on thrust forces and bushing shapes

For the experiment conducted to determine the lower die effect on the axial thrust forces as well as the geometry of the bushing shape, the workpiece is fixed in the novel-designed fixture when the friction drilling process is operated. The 1.25 mm thick aluminum alloy sheet metals is used as the work material. The experiment is conducted at 4000 rpm spindle speed, 3.81 cm/min feed rate using 5.3 mm diameter friction drill bit with drill paste on the surface of the tool.

The following figures illustrate the experimental data of axial thrust forces in friction drilling with lower die compared to the same input parameters and work material friction drilling with no lower die. Two designs in different dimensions as shown in Table 6 of stepped-holes in lower die are carried out in the experiment. The horizontal axis represents the time from initial contact between the drill bit and the work material in the unit of millisecond. The vertical axis represents the axial thrust forces during the friction drilling process in the unit of Newton.

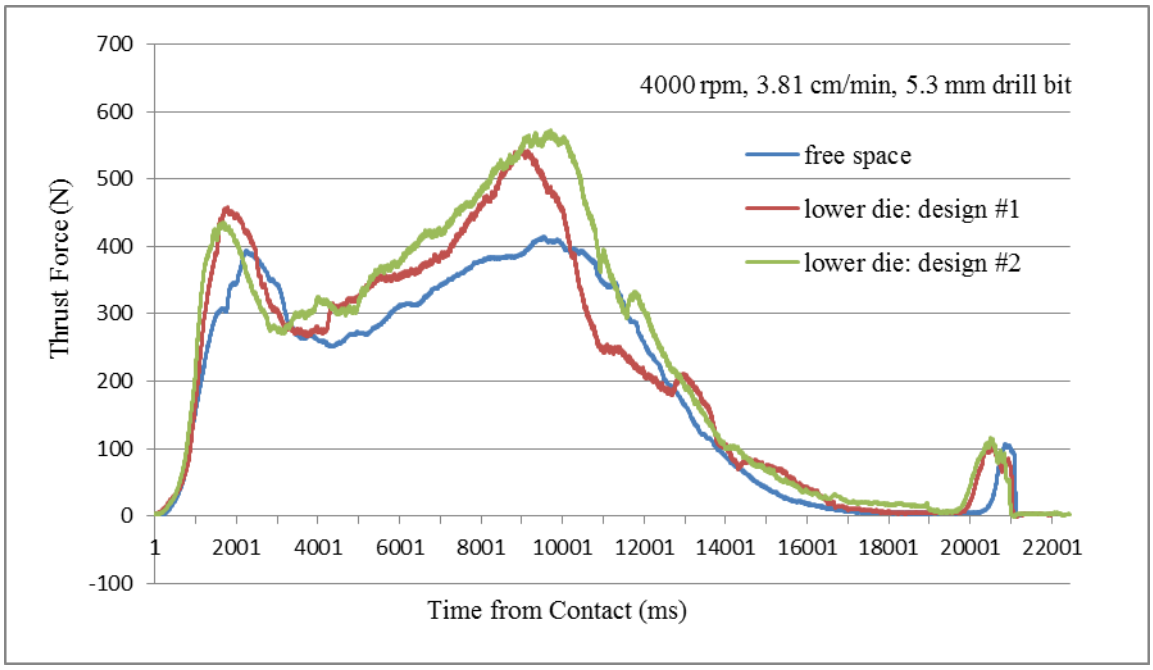

Figure 32: Comparison between free space and two designs of lower die friction drilling at 4000 rpm spindle speed and 3.81 cm/min feed rate using 1.25 mm thick aluminum workpieces and 5.3 mm diameter drill bit.

Based on the data in Figure 32, it is observed that the thrust force is higher in friction drilling process with the lower die. Both the peak values uplift and shift left compared to the original free space friction drilling. With the lower die constraining the work material, it is reasonable that larger thrust forces are needed. The platform surface of the lower die supports the entire workpiece to prevent it from large deflection, therefore, higher reaction forces acting on the workpiece results in larger thrust forces. The shifting of the thrust force curve towards left indicates an earlier interaction between the friction drill bit and the work material. The workpiece is better supported than the original fixture. Therefore, the transition points on the curve happen earlier in the lower die friction drilling.

After the second peak on the thrust force curve, the work material is already penetrated. At the same time, the formation of bushing is still in progress. The designed stepped-hole plays an important role in the forming shape of the bushing. A strong and complicated interaction between the bushing material and the stepped-hole of lower die makes the drop force after the second peak more irregular than original free space friction drilling. In addition, the varying dimensions of the confined spaces make the force curve rise and fall at slightly different time.

5.3.2 Effect of input variables in lower die friction drilling

To determine the effect that different input variables have on the axial thrust forces in lower die friction drilling, the experiments of run 1 to run 3 are designed. The 1.25 mm thick aluminum alloy sheet metal is used as the work material. The

experiments are conducted in 5.3 mm diameter friction drill bits with drill paste on the surface of the tool.

Table 7 shows the experiment run matrix in lower die friction drilling. Runs of experiment, labeled as 1-3 are executed to study the effect of different variables. The experiments are designed to study the effect of spindle speeds and feed rates on the thrust force curves. The experiments conducted with a variety of combination of input parameters are described in Table 7.

Table 7: Different input variables in lower die friction drilling experiments.

Experiment/run	Workpiece thickness (mm)	Tool diameter (mm)	Spindle speed (rpm)	Feed rate (cm/min)
1	1.25	5.30	4000	3.81
2	1.25	5.30	4000	6.35
3	1.25	5.30	3000	6.35

The following chart presents the experimental data of axial thrust forces in comparison of different input variables in original free space and lower die friction drilling. The horizontal axis represents the time from initial contact between the drill bit and the work material in the unit of millisecond. The vertical axis represents the axial thrust forces during the friction drilling process in the unit of Newton.

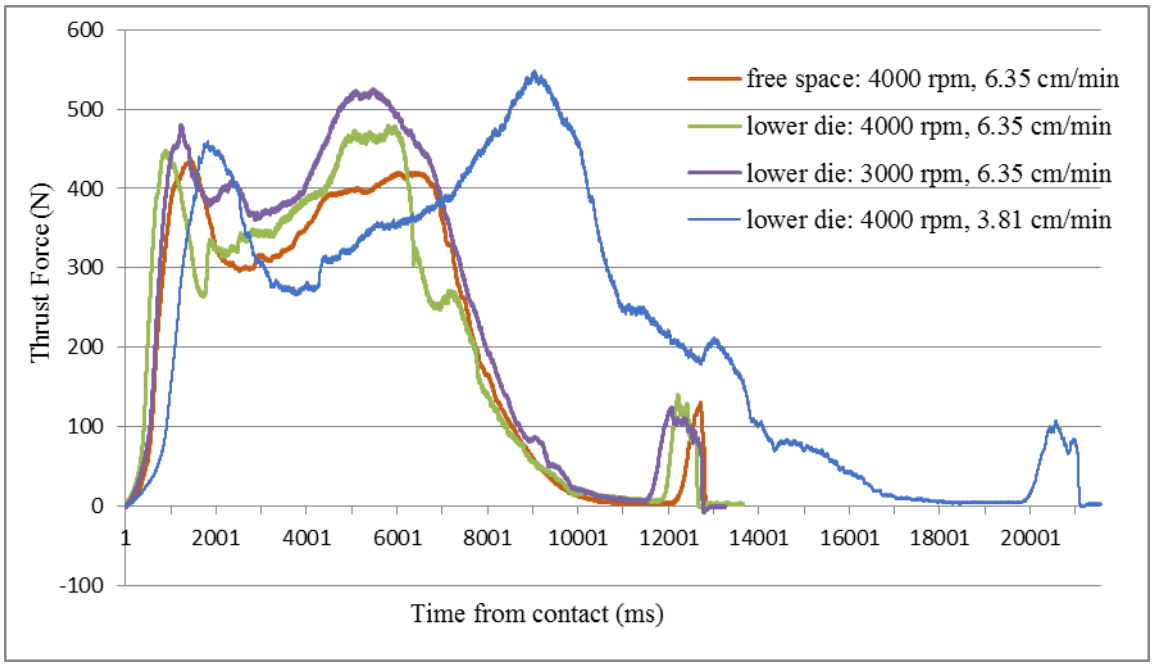

Figure 33: Comparison of free space and lower die friction drilling with different spindle speeds and feed rates using 1.25 mm thick workpiece and 5.3 mm diameter drill bit.

Based on the data in Figure 33, the thrust force curves in lower die friction drilling present the typical trend but with some irregular vibration. The complex interaction in the work material, the friction drill bit, and the stepped-hole in lower die causes the unpredictable oscillation. In general, the curves with lower die are shifted to the left of the curve with free space. The overall required thrust forces are larger with lower die. The discrepancy is due to the constraint of the workpiece to the fixture, as discussed in section 5.3.1.

The spindle speed and feed rate effects on the thrust force curve remain the same as original free space friction drilling. Regarding the comparison between 4000 rpm

spindle speed with 6.35 cm/min feed rate and 3000 rpm with 6.35 cm/min in lower die friction drilling, the required thrust force at high spindle speed is generally lower. The thrust force curve at 4000 rpm spindle speed with 3.81 cm/min feed rate in lower die friction drilling shifts noticeably to the right of the other curves due to its lower feed rate. Nevertheless, the force curve of the lowest feed rate at 3.81 cm/min in lower die friction drilling does not show the consistent result of smaller required thrust forces. The error in locating the center of the stepped-hole to produce a friction drilled hole is likely an issue. In addition, to achieve a predictable result, the more accurate design and manufacture of the stepped-hole in lower die is needed.

5.4 Sample characterization results of lower die friction drilling

The axial thrust force curves from different spindle speeds, and feed rates in lower die friction drilling experiments have been investigated. Qualitative sample characterization results are shown and discussed in the section. To evaluate the quality of holes in friction drilling, the shape of bushing is an important criterion. The quality of bushing shape is observed and judged via cylindricality, effective length, cracks, and petal formation [9].

The specimens are prepared for microscopy examination in the same manner as previous section. The workpieces with the friction drilled hole are sheared by the cutting blade at the center of the hole. The cross-sectioned edge of the workpiece is manually polished using finer sand papers progressively. The preparation facilitates the optical microscopy examination. Dino-Lite digital microscope is used to capture the cross-

sectioned images of the friction drilled workpieces from effective views. The cross section view of the bushing shape is presented to compare different features of the bushings.

The following figures show low magnification optical images of the cross-sectioned workpieces. The photomicrographs present the cross-sectional view parallel to the polished plane which is feasible to examine the most information of the bushing feature. The material of the polished specimens is 1.25 mm thick aluminum alloy sheet metal. The effect of lower die on the shape of bushing and the hole geometry is discussed. The selected drilling parameters are 4000 rpm spindle speed with 3.81 cm/min feed rate conducted with 5.3 mm diameter friction drill bit attaching drill paste on the surface of the tool. Some distinct geometry such as length of bushing, cracking, petal formation, and denting of the workpieces resulted from different drilling parameters are able to be observed in the photomicrographs.

Friction drilling is capable of displacing work material to form increased thickness called bushing. The bushing allows for stronger fastening the thin-walled profiles, sheet metal, or tubing to make it simple to joint devices efficiently. To cut the threads inside the friction drilled hole become one of the solutions to attach devices to the thin-walled profiles in current manufacturing industry. Therefore, it is practical to tap the threads in the friction drilled hole to evaluate the performance of the improved holes in the study. Referring to the metric thread size & tap drill table, the M6×1.0 and M8×1.25 tap sizes are selected for the diameter of 5.3 mm and 7.3 mm friction drilled hole, respectively. A hand-tapper is held skillfully perpendicular to the workpiece

clamped at the fixture to cut good threads. Via the handlebar, the hand-tapper is rotated clockwise manually throughout the bushing material. The same technique for preparing microscopy specimen is utilized to obtain the cross section of the threaded bushing shapes.

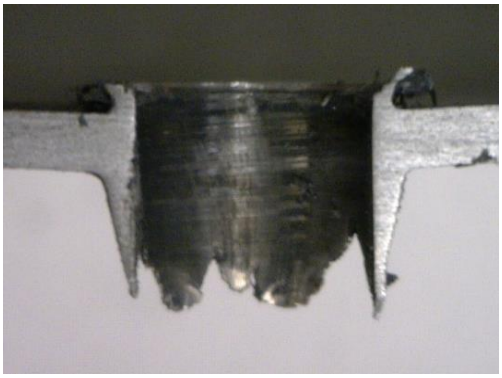

(a) Cross section of the bushing shape.

Figure 34: The original free space friction drilled holes are formed at the same input parameter as 4000 rpm spindle speed and 3.81 cm/min feed rate. (a) The cross section of the bushing shape. (b) The cross section of the bushing shape with threads tapped.

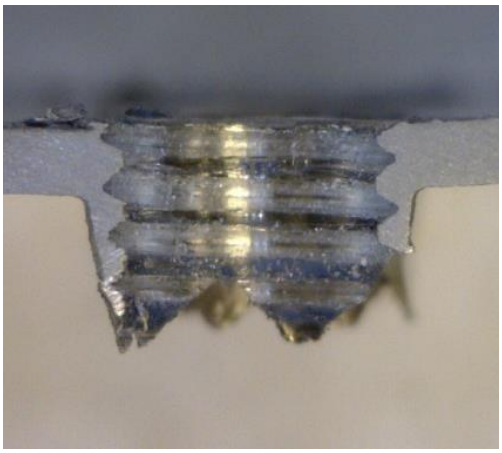

(b) Cross section of the bushing shape with threads tapped.

Figure 34: Continued.

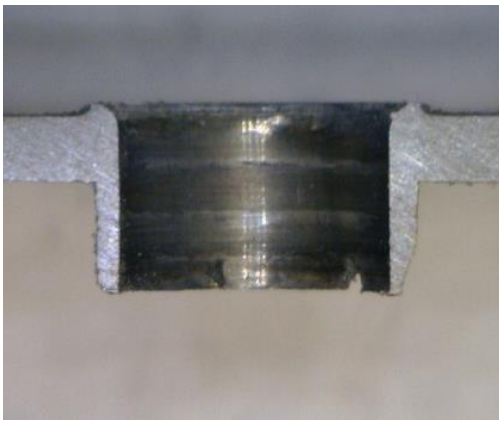

(a) Cross section of the bushing shape.

Figure 35: The lower die friction drilled holes are formed at the same input parameter as 4000 rpm spindle speed and 3.81 cm/min feed rate. (a) The cross section of the bushing shape. (b) The cross section of the bushing shape with threads tapped.

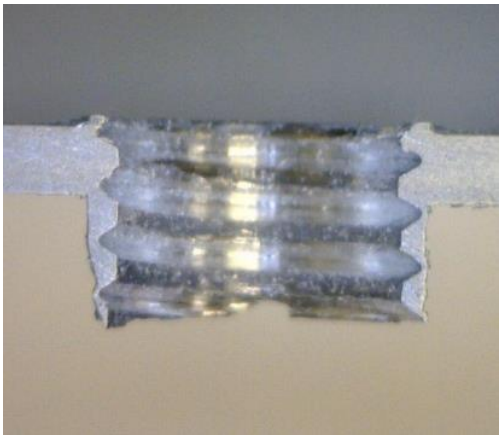

(b) Cross section of the bushing shape with threads tapped.

Figure 35: Continued.

Figure 34 and Figure 35 show the cross-sectional views in original free space and lower die, respectively, friciton drilling 1.25 mm thick aluminum alloy workpieces at 4000 rpm spindle speed with 3.81 cm/min feed rates. The 5.3 mm diameter friciton drill bit is carried on with drill paste on the surface of the tool. The cross-sectioned views are meaningful in revealing different features of the friction drilled hole area clearly. Without the control of lower die in bushing forming, the cracks and petal formation destroy the useful surface area to limit the loading capability for hole threading. These undesirable bushing features such as cracks, petal formation in friciton drilling sheet metals negatively influence the effective length and strength for threading. The effective thread count in original free space friction drilled hole shown in Figure (b) is merely two.

In Figure 35, the benefit of lower die in improving bushing shape is clearly demonstrated. The cracking and petal formation are nearly dissappeared. Compared to

the gradually-thinned bushing material in original free space friciton drilling, the bushing material in lower die is formed cylindrically and uniformly in its thickness providing more strength for screw threading. The fracture in the thinner part of the bushing material while the threads are tapped does not appear in lower die bushing. The effective threads in lower die friction drilled hole shown in Figure 35 (b) is in complete three cycles. The additional thread count indicates fifty percent improvement of the thread performance in lower die bushing shape.

However, some improvement in producing threaded friction drilled holes with higher quality can still be further investigated. First, to achieve the goal of making more uniform bushing thickness, the manufacturing of the steps in the confined space with two different diameters of the twist drill bits at the identical center is the key point. Also, in experiment, efforts can be made to precisely locate the friction drill bit at the center of the stepped-hole. Second, the coaxial problem of accurately aligning the hand-tap with the friction drilled hole needs to be improved. It is necessary to make the hand-tap aligned as perfectly as possible, so the thickness of the threaded hole will be consistent throughout the bushing material. If the alignment task is not completed initially, the error will magnify as the depth goes further. The fact is that once the first or second thread is cut, the tapping angle is already established throughout the hole.

6. JOINING PROCESS IN FRICTION DRILLING

6.1 Introduction

Friction stir welding (FSW), a solid state joining operation, has a similar concept to friction drilling [31]. Solid state welding is a collective of welding processes. It produces coalescence of workpieces at temperatures below the melting point of the base work materials being joined [32]. Friction stir welding process has been developed by The Welding Institute in Cambridge, United Kingdom in 1991. With a rotating tool generating frictional heat, the process led to the joining of separate workpieces [33]. Friction stir welding created materials coalescence by the mechanically-induced frictional heat between rubbing surfaces [34, 35]. Once the sufficient heat reaches, the fusion in the work materials starts to hold them together under additional pressure. The significant difference between friction stir welding and friction drilling is that the former creates frictional heat and softens the work materials to join them, while the latter also creates frictional heat and softened work material to deform a hole with bushing. Due to the similarities in two processes, it could be possible to join two sheet metals with one simple friction drilling operation. If successful, it is a time-saving approach to attach two thin-walled workpieces even without threading and screws.

In this section, the feasibility of joining double sheet metals in friction drilling will be explored. The double-layer friction drilling experiments is carried on with both original free space fixture and designed stepped-hole lower die.

The novel double-layer friction drilling experiments are conducted with selected input parameters. The axial thrust forces under different parameters are measured and the geometries of the bushing shapes are observed. The friction drilling forces are collected by utilizing the dynamometer as well as LabVIEW SignalExpress data acquisition system. The voltage signal is recorded continuously with the selected sampling rate of 1000 Hz, and finally applied to Voltage-Newton calibration equation. The bushing shape geometries are presented by cross-sectional view in photomicrographs. Dino-Lite digital microscope is used to capture the cross-sectional images of the friction drilled holes with better magnification and resolution.

6.2 Double sheet metals friction drilling experiments

The original free space fixture in section four is adopted. The change is that single workpiece is replaced by double stacked workpieces when friction drilling process is operated. The workpieces used are aluminum alloy 6061-T651 with the thickness of 1.25 and 2.29 mm, and secured firmly by the bolts and clamping bars in the shallow step. This fixture is mounted on the dynamometer on the CNC milling machine for measuring the forces.

Table 8 shows the experiment run matrix in double-layer friction drilling. Runs of experiment, labeled as 1-4 are carried out to study the effect of different variables. The experiment runs for 1-2 and 3-4 are designed to study the effect of spindle speeds and feed rates on the thrust forces with the combination of different workpiece

thicknesses (1.25 mm and 2.29 mm.) The experiments conducted with a variety of combination of input parameters are described in Table 8.

Table 8: Different parameters applied in double-layer friction drilling experiments.

Experiment/run	Upper workpiece (mm)	Lower workpiece (mm)	Drill bit diameter (mm)	Spindle speed (rpm)	Feed rate (cm/min)
1	1.25	1.25	5.3	4000	3.81
2	1.25	1.25	5.3	3000	6.35
3	2.29	1.25	5.3	4000	3.81
4	2.29	1.25	5.3	3000	6.35

6.2.1 Double- layer effect on thrust forces and bushing shapes

To determine the double-layer effect on the axial thrust forces as well as the geometries of the bushing shape, double stacked workpieces are fixed in the original free space fixture to operate friction drilling process. With the 1.25 mm thick layer at the bottom, the 1.25 mm and 2.29 mm thick workpieces are selected as the top layer. Based on the experimental results in section four, it is noticed that both increase in spindle speed and decrease in feed rate result in decrease in the thrust force. With lower thrust force, the workpiece deflects less and the tool life lengthens [6]. Therefore, 4000 rpm

spindle speed, and 3.81 cm/min feed rate are selected as input parameters. The 5.3 mm diameter friction drill bit is used with drill paste on the surface of the tool.

The following figures illustrate the experimental data of axial thrust forces compared to the same input parameters in single sheet friction drilling. The horizontal axis represents the time from initial contact between the drill bit and the work material in the unit of millisecond. The vertical axis represents the axial thrust forces during the friction drilling process in the unit of Newton.

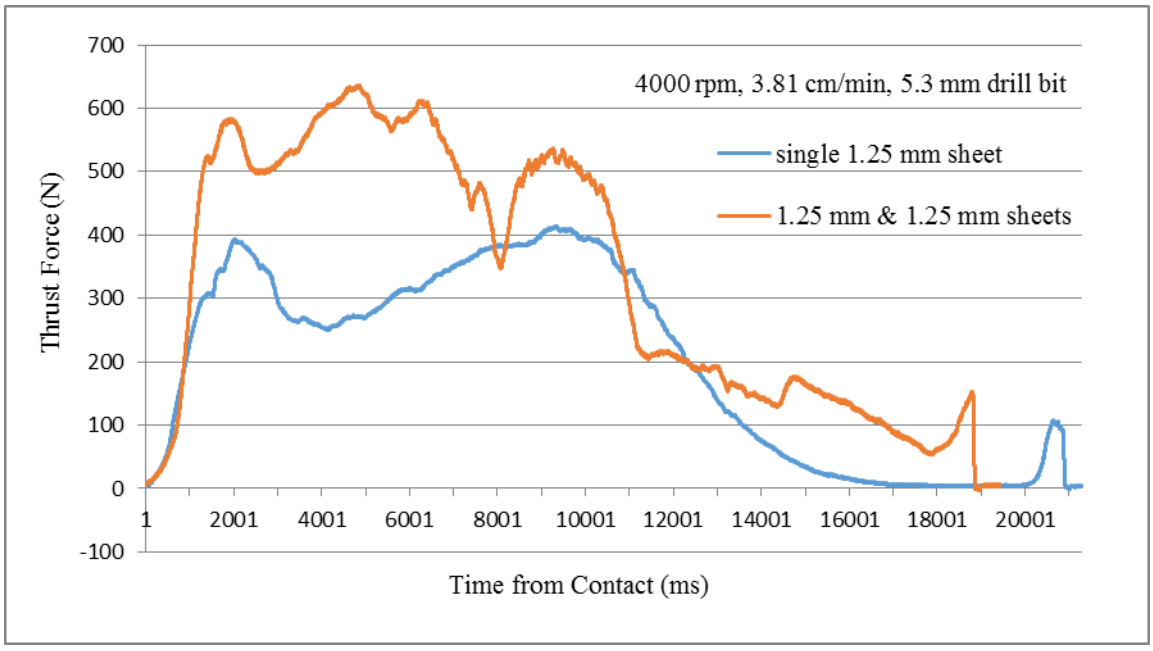

Figure 36: Comparison of thrust force curves between single 1.25 mm sheet and double 1.25 mm sheets at 4000 rpm, 3.81 cm/min.

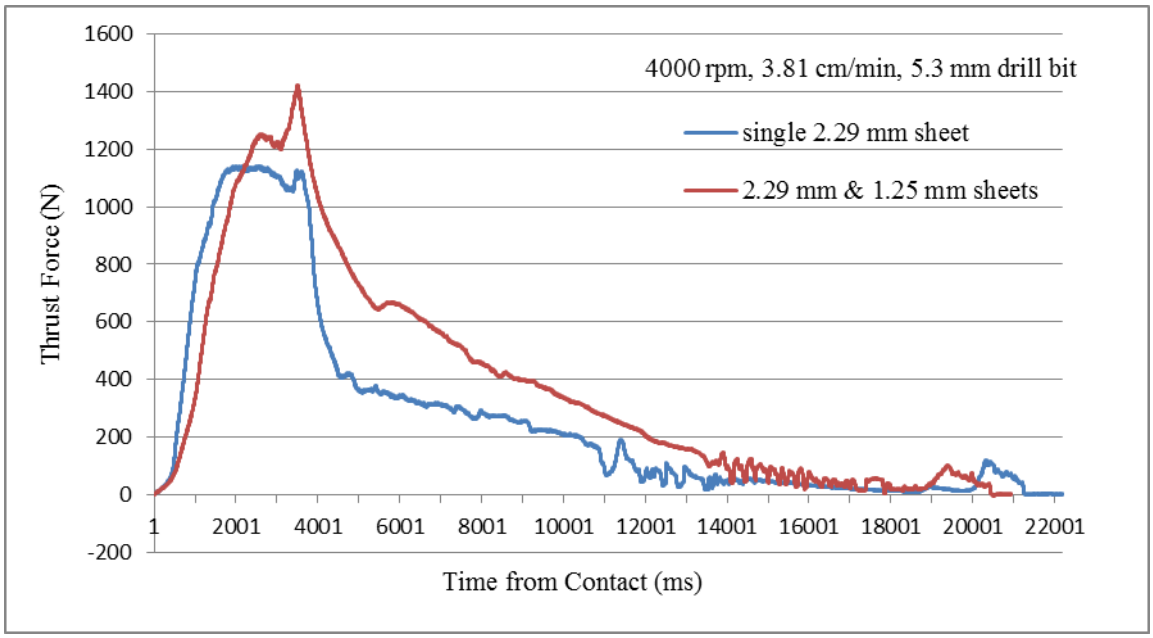

Figure 37: Comparison of thrust force curves between single 2.29 mm sheet and 2.29 mm & 1.25 mm sheets at 4000 rpm, 3.81 cm/min.

The measured thrust forces of experiment run 1 and 3 in friction drilling double aluminum alloy sheet metals are compared to the same input parameters in friction drilling single sheet metal are shown in Figure 36 and Figure 37. It can be observed that larger thrust force is required in friction drilling process while the 1.25 mm thick workpiece is added. At 4000 rpm spindle speed, and 3.81 cm/min feed rate, the largest thrust force peak values are 623 N and 407 N for double 1.25 mm sheets and single 1.25 mm sheet, respectively. At the same input variables, the thrust force peak values are 1377 N and 1103 N for 2.29 mm & 1.25 mm sheets and single 2.29 mm sheet, respectively. Since the bottom layer firmly supports the softened work material and

confines the forming space for bushing material, it is reasonable for the thrust forces to increase.

The shorter process time is required in double-layer friction drilling compared to single layer friction drilling. At the same feed rate, it takes 18.8 seconds and 21.0 seconds to complete the friction drilling process in double 1.25 mm sheets and single 1.25 mm sheet, respectively. Further, 20.2 seconds and 21.2 seconds are required to complete the friction drilling process in 2.29 mm & 1.25 mm sheets and single 2.29 mm sheet, respectively. The reason for the reduction of time for the whole friction drilling process is due to the displacement of the contact point. More bending deflection in the sheet metal workpiece is observed in the single layer condition, although the fixture is designed to prevent excessive bending. With the second workpiece below, the top workpiece is better supported to avoid bending in the downward direction. In fact, the work area of the top layer is deformed into a convex shape due to the formation of bushing and support of the second layer. The effect of temperature-dependent mechanical properties is likely the main reason. During the friction drilling process, the increase of the workpiece temperature results in low stiffness of the material. The top layer work material becomes easier to deform, while the lower layer still maintains at relatively lower temperature which is more difficult to bend. Therefore, under the constant feed rate, the shorter period of time is required from the tip of drill bit contacting the workpiece to the shoulder trimming the boss material in double-layer condition.

Due to a slight convex geometry created at the work area of the top layer, it is necessary to reset and adjust the defined stop end position. The cutting blade of the Long Flat 5.3 Flowdrill© friction drill bit is designed to contact the workpiece surface to allow a removal of the boss. The precise setting of the stop end position is required to prevent overcutting of the collar, otherwise, the tool and machine may be damaged due to overloading.

6.2.2 Effect of input variables in double-layer friction drilling

To determine the effect that different input variables have on the axial thrust forces as well as the geometries of the bushing shape, the experiments of run 2 and run 4 shown in Table 8 are designed. The 1.25 mm and 2.29 mm thick aluminum alloy sheet metals are used as the work material. The experiments are conducted in 5.3 mm diameter friction drill bit with drill paste on the surface of the tool.

The following figures present the experimental data of axial thrust forces compared to different input variables in double-sheet friction drilling. The horizontal axis represents the time from initial contact between the drill bit and the work material in the unit of millisecond. The vertical axis represents the axial thrust forces during the friction drilling process in the unit of Newton.

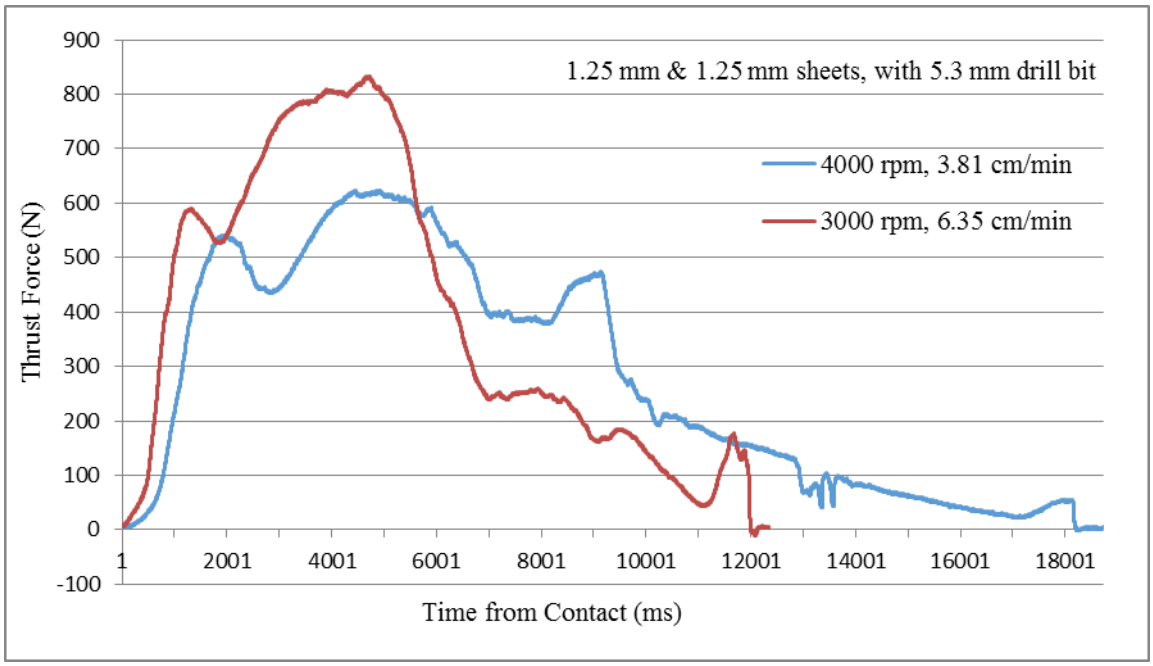

Figure 38: Comparison of thrust force curves between 4000 rpm with 3.81 cm/min and 3000 rpm with 6.35 cm/min in friction drilling double 1.25 mm sheets using 5.3 mm drill bit.

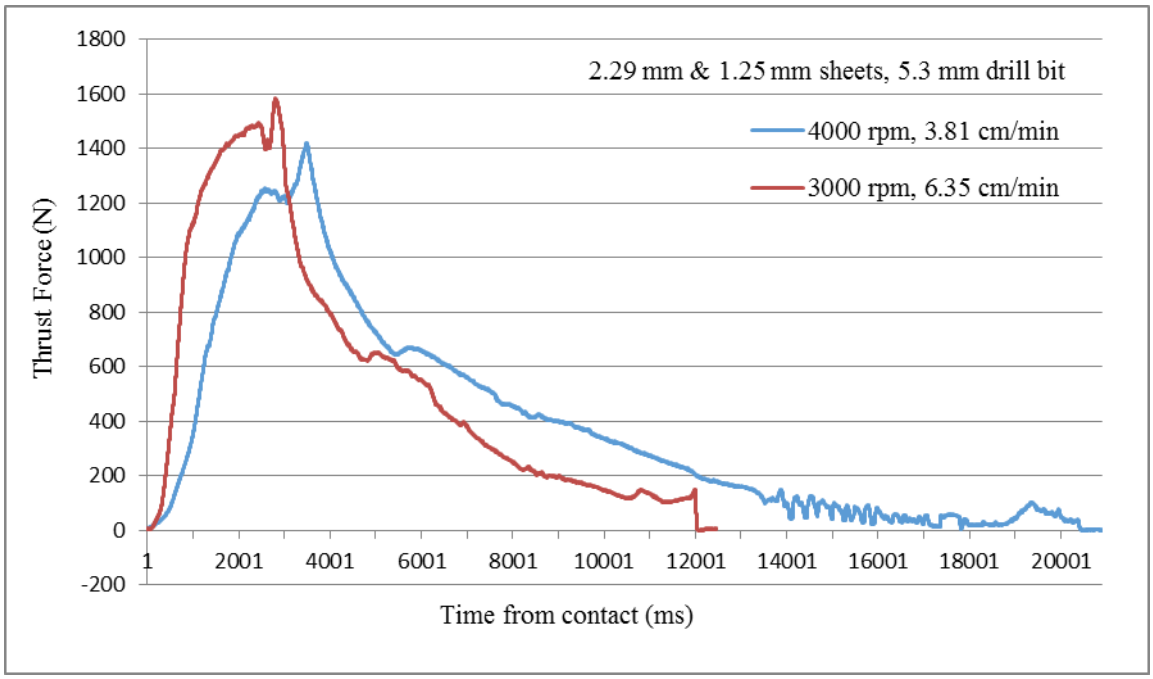

Figure 39: Comparison of thrust force curves between 4000 rpm with 3.81 cm/min and 3000 rpm with 6.35 cm/min in friction drilling 2.29 mm & 1.25 mm sheets using 5.3 mm drill bit.

The measured thrust forces of experiment run 2 and 4 for friction drilling of aluminum alloy sheets are compared to experiment run 1 and 3 of different input parameters in double-sheet friction drilling shown in Figure 38 and Figure 39. In both cases, the increase of the thrust forces can be observed when changing from 4000 rpm spindle speed with 3.81 cm/min to 3000 rpm spindle speed with 6.35 cm/min feed rate.

In the case of joining two 1.25 mm sheets, the peak values of the thrust force are 830 N and 623 N under 3000 rpm spindle speed with 6.35 cm/min feed rate and 4000 rpm spindle speed with 3.81 cm/min feed rate, respectively. In case of joining 2.29 mm &1.25 mm sheets, the peak values of the thrust force are 1541 N and 1377 N under 3000

rpm spindle speed with 6.35 cm/min feed rate and 4000 rpm spindle speed with 3.81 cm/min feed rate, respectively. Based on the results in section four, with the aim to reduce the thrust forces in friction drilling process, either the increase of tool spindle speed or the decrease of tool feed rate plays an essential role. The thrust force graphs of double-layer friction drilling show the consistent results that with the increase of spindle speed and the reduction of feed rate, the required thrust forces decrease desirably as well.

6.3 Sample characterization results of double-sheet friction drilling

The qualitative sample characterization results of different parameters in double-sheet friction drilling for joining are shown and discussed in the section. Other than evaluating the bushing shape quality in friction drilling, the focus is on the joining of the two sheet metals at friction drilled hole.

The double-layered workpieces with the friction drilled hole are sheared by the cutting blade at the center of the hole. The cross-sectioned edge of the workpiece is manually polished using sand papers. Dino-Lite digital microscope is used to capture the cross-sectioned images of the friction drilled workpieces from effective views. The cross-sectional view of the friction drilled hole is presented to compare the features of the material coalescence.

Different coalescence situations are noticed in double-sheet friction drilling. In the case of 2.29 mm & 1.25 mm sheets, two workpieces are successfully bonded by the bushing material at the top layer in both 4000 rpm spindle speed with 3.81 cm/min feed rate and 3000 rpm spindle speed with 6.35 cm/min conditions. Whereas, the case of

double 1.25 mm sheets friction drilling indicates more complex coalescence results. Two workpieces remain diffuse-bonded at 4000 rpm spindle speed with 3.81 cm/min feed rate drilling condition, yet they no longer join together at 3000 rpm spindle speed with 6.35 cm/min feed rate.

It is evident to find a coarse bore surface finish with scoring damages especially in the lower section of the aluminum alloy friction drilled hole. Due to the depletion of drill paste for the entire process, the lower section is considered as friction drilling by the drill bit alone. The interior surface shows the typical features of extensive plastic deformation with delamination and abrasion in friction drilling aluminum alloy [20, 36, 37].

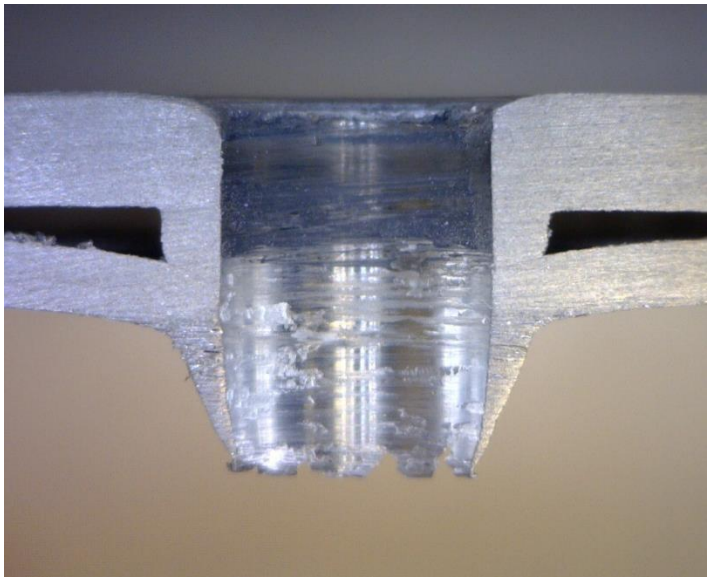

Figure 40: The coalescence of 2.29 mm & 1.25 mm sheet metals in free space friction drilling at 4000 rpm and 3.81 cm/min using 5.3 mm drill bit.

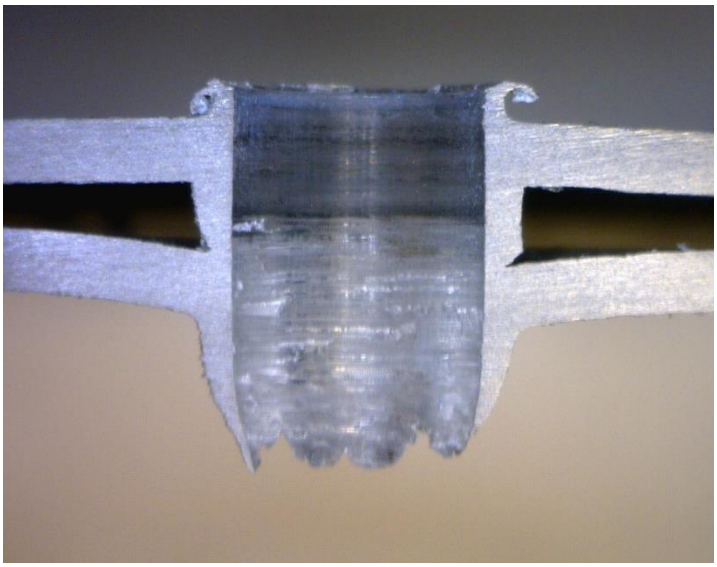

Figure 41: The coalescence of double 1.25 mm sheet metals in free space friction drilling at 4000 rpm and 3.81 cm/min using 5.3 mm drill bit.

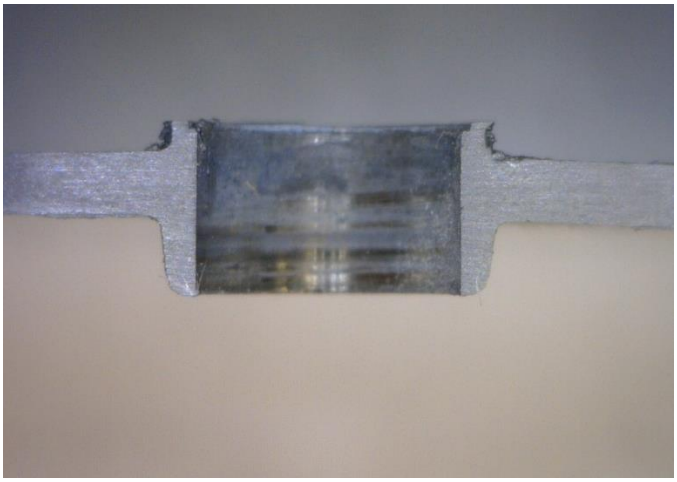

Figure 42: The upper sheet of free space friction drilling double 1.25 mm sheet metals at 3000 rpm with 6.35 cm/min.

Under the 3000 rpm spindle speed with 6.35 cm/min feed rate condition of friction drilling to join two 1.25 mm sheet metals, the process failed to achieve bonding. The two sheet metals separate from each other after the friction drilling process completes.

While failed in joining, it is discovered that the upper layer has an excellent quality of the well-cylindrical bushing shape without any crack and petal formation. The flexibility of the sheet metals allows the bushing to form between layers. Due to the limited space, the bushing material is constrained, and therefore, the perfect bushing shape without any petal and crack is produced. While the bottom layer makes significant contributions to the shape of bushing, it becomes a piece of sacrificial material with no functionality.

6.4 Joining sheet metals by friction drilling with the lower die

To improve the joining quality in double-layer friction drilling, attempts were made to use a lower die. The lower die is expected to confine the deflection and deformation of the bottom workpiece, and therefore, a better bonding between two layers could be achieved. On one hand, the gap between two work materials is anticipated to shrink after the drilling. On the other hand, the promoting joint probability is foreseeable in double-sheet friction drilling under multiple input parameters.

To determine the effect of the lower die on joining, the experiments of Run 1 to Run 4 shown in Table 9 are conducted. The input parameter of 4000 rpm spindle speed and 3.81 cm/min feed rate is selected based on the low thrust forces and better bushing shapes observed from the previous study. The 1.25 mm and 2.29 mm thick aluminum alloy sheet metals are used as the work material. The experiments are conducted in 5.3 mm diameter friction drill bits with drill paste on the surface of the tool.

Table 9: The parameters of double-layer friction drilling with the lower die.

experiment	Upper workpiece thickness (mm)	Lower workpiece thickness (mm)	d_1 (mm)	d_2 (mm)	h (mm)
1	1.25	1.25	5.30	6.40	2.80
2	1.25	1.25	5.30	6.60	3.00
3	2.29	1.25	5.30	6.70	3.10
4	2.29	1.25	5.30	7.00	3.50

The following chart presents the experimental data of axial thrust forces in comparison of same input variable between original free space and lower die in double-layer friction drilling. The horizontal axis represents the time from initial contact between the drill bit and the work material in the unit of millisecond. The vertical axis represents the axial thrust forces during the friction drilling process in the unit of Newton.

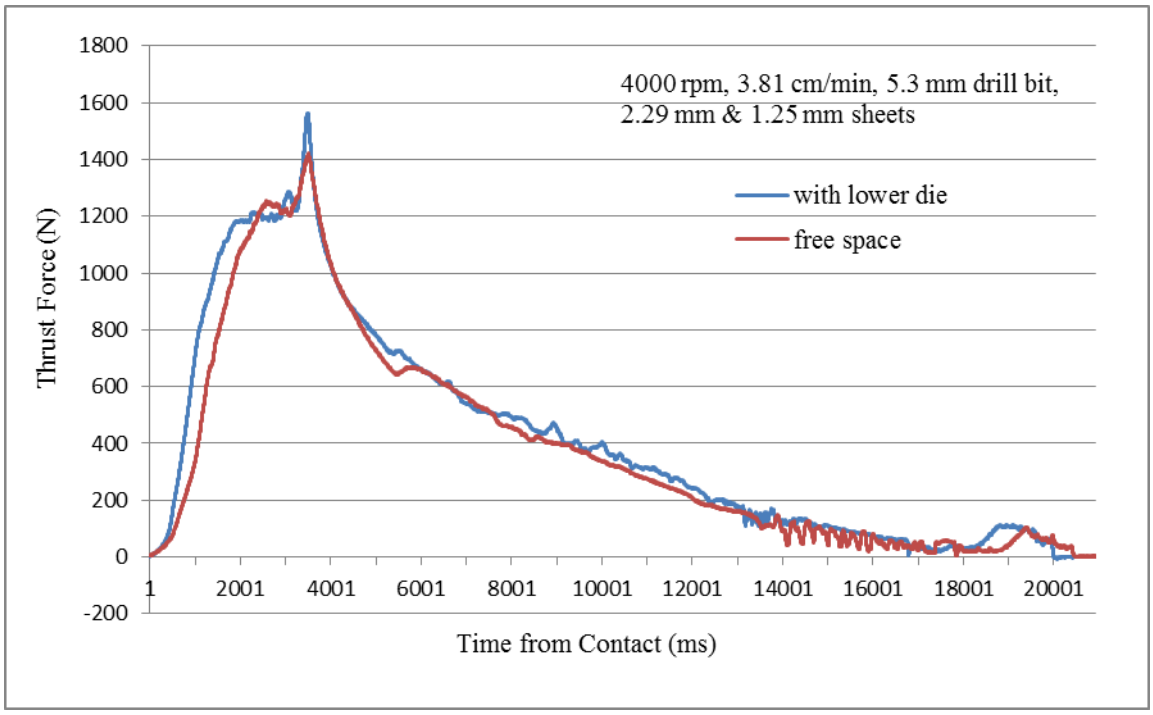

Figure 43: Force curves of friction drilling 2.29 mm & 1.25 mm sheets compared between lower die and original free space fixture at 4000 rpm, 3.81 cm/min using 5.3 mm drill bit.

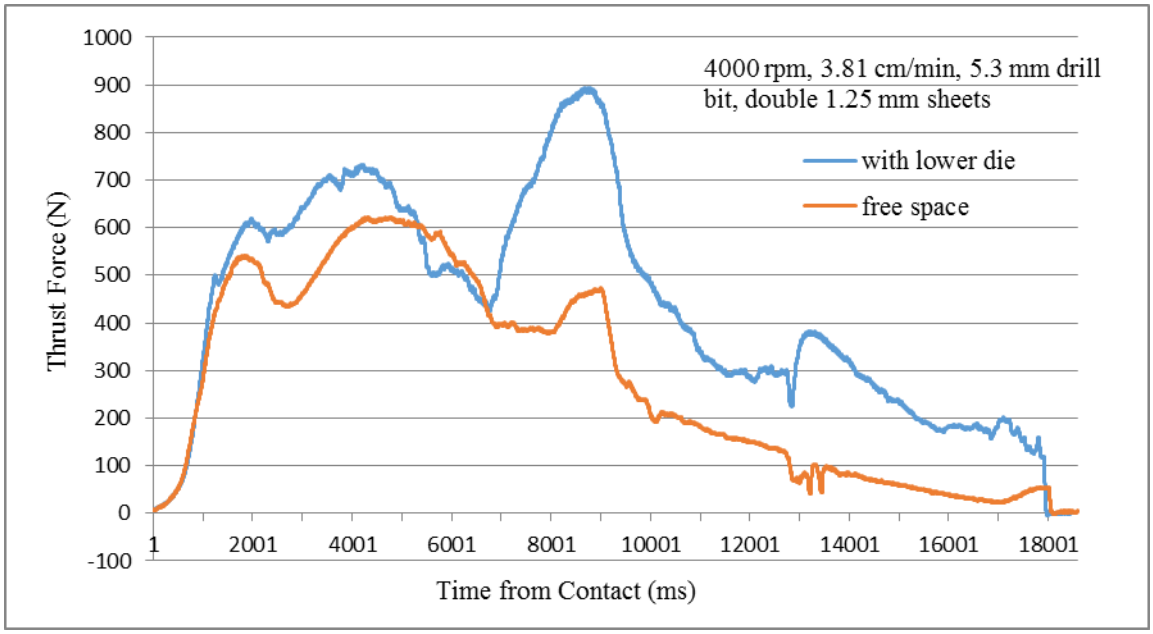

Figure 44: Force curves of friction drilling double 1.25 mm sheets compared between lower die and original free space fixture at 4000 rpm, 3.81 cm/min using 5.3 mm drill bit.

In Figure 43 and Figure 44, the measured thrust forces of lower die friction drilling 2.29 mm & 1.25 mm aluminum alloy sheets and double 1.25 mm aluminum alloy sheets are respectively compared to original free space friction drilling at 4000 rpm spindle speed with 3.81 cm/min feed rate using 5.3 mm diameter friction drill bit.

Based on both charts, the thrust force curves in lower die friction drilling follows the typical trend as those in original free space but with some irregular vibration. The complex interaction in the double-layered work materials, the friction drill bit, and the stepped-hole in lower die causes the oscillation. In general, the thrust force with lower die increases at a higher rate to the first peak, which indicates a shorter period of time is needed to reach the first thrust force peak. Moreover, the shorter period of time is

required in joining with lower die compared to friction drilling with no lower die. The overall required thrust forces are larger with lower die. The difference is due to the constraint of the lower die fixture.

Similarly, due to a convex generated at the work area of the top layer, it is necessary to reset and adjust the end position to the tool. The precise setting of the position is required to prevent overcutting of the collar. With wrong setup, the tool and machine may be damaged due to overload.

6.5 Sample characterization results of joining by friction drilling with lower die

The qualitative sample characterization results of using lower die and original free space for joining are shown and discussed in the section. The double-layered workpieces with the friction drilled hole are sheared by the cutting blade at the center of the hole. The cross-sectioned edge of the workpiece is manually polished using sand papers. Dino-Lite digital microscope is used to capture the cross-sectioned images of the friction drilled workpieces from effective views. The cross-sectional view of the friction drilled hole is presented to compare the features of the material coalescence, and the denting of the workpieces.

Noticeable results are found in sheet metals coalescence in double-sheet lower die friction drilling. In the case of 2.29 mm & 1.25 mm sheets, two workpieces are successfully bonded at 4000 rpm spindle speed with 3.81 cm/min feed rate using lower die fixture. Whereas, the case of double 1.25 mm sheets friction drilling has different coalescence results. At 4000 rpm spindle speed with 3.81 cm/min feed rate using lower

die fixture, the workpieces no longer join together. With the lower die fixture, it is apparent that the deflection of bottom layer has been reduced. The convex at the work area in the top layer is essential to the result of joint. Due to the larger stiffness of the 2.29 mm thick sheet metal, a small deflection in convex shape is observed in the top layer. Therefore, the coalescence results remain the same no matter lower die is used.

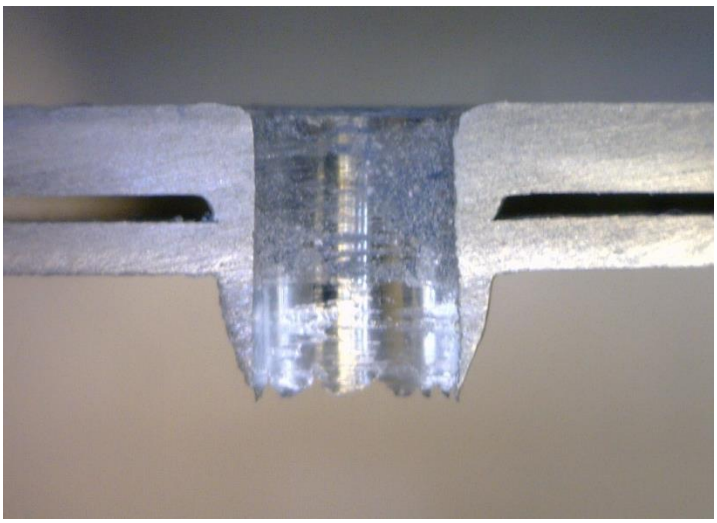

Figure 45: The coalescence of 2.29 mm & 1.25 mm sheet metals in lower die friction drilling at 4000 rpm and 3.81 cm/min using 5.3 mm drill bit.

While the top layer is replaced by 1.25 mm thick sheet metal, the difference becomes significant. A more obvious convex shape at the work area in the top layer is observed, when the lower die is applied. During the friction drilling process, the increase of the workpiece temperature causes the stiffness of the material to reduce. The top layer

work material is inclined to deflect. At the same time, the lower die-confined bottom layer at relatively lower temperature resists the bottom layer to bend. Due to the excessive deflection in the top layer, the sheet metals are less likely to bond.

7. CONCLUSIONS AND FUTURE WORK

This experimental study investigated friction drilling process parameters and explored novel methods to improve the bushing shape of the friction drilled holes. More than a hole-making process, friction drilling has also been experimented as a joining process for thin sheet metals.

7.1 Conclusions

The work conducted in the research of friction drilling contributed to the following conclusions:

- Tests were conducted to obtain thrust force results and friction-drilled holes cross-sectional images at various stages of friction drilling process. At the initial stage, the thrust force rapidly increased as the center part of the drill bit engaged in mechanical indentation of the workpiece. Thrust force dropped as penetration occurred. The conical part of the tool contributed to form the bushing, and the cylindrical part of the tool configured the complete hole diameter. The better understanding of the thrust force curve was established to explain two types of thrust force curves when drilling material with different thicknesses in the experiment.
- The parametric study in axial thrust force indicated that either increasing spindle speed or decreasing feed rate can reduce the magnitude of the thrust force. However, the combination effect of spindle speed and feed rate within

the studied range implied the former had more dominant influence on the thrust force than the latter.

- The designed lower die fixture is able to improve the bushing shape by its cylindricality, cracks, and petal formation in friction drilling process. Threads were tapped to demonstrate the improvement of the bushing shape in practical application.
- The potential of joining thin-walled profile in friction drilling process has been explored. Different coalescence situations are noticed in double-sheet friction drilling. At 4000 rpm spindle speed with 3.81 cm/min feed rate, both 2.29 mm & 1.25 mm sheet metals and double 1.25 mm sheets were bonded. Whereas, at 3000 rpm spindle speed with 6.35 cm/min feed rate, only 2.29 mm & 1.25 mm sheet metals were successfully joined. While joining two 1.25 mm sheets were not successful, unexpectedly the process created a high quality bushing without any cracks or petal formation.

7.2 Future work

The following future work is suggested:

- Microstructure observation associated with bushing shape improvement and joined workpieces can be investigated. High temperature generated by large friction force leads the workpiece material to soften and deform. The material properties and microstructures alter during the process. The alternation associated with bushing shapes and coalescence can be further investigated.

- The finite element (FE) modeling can be used to study stress, strain, temperature, and material flow during friction drilling process. FE modeling can also benefit the design of the tool geometry, and the selection of tool material to extend the tool life.
- The FE modeling can simulate lower die friction drilling process. The further development in FEM can improve the precision in designing the stepped-hole. It can also help to avoid tool damage, due to the large material deformation in friction drilling.

REFERENCES

[1] Streppel, A. H., and Kals, H. J. J., 1983, "Flowdrilling: a preliminary analysis of a new bush-making operation," Annals of the CIRP, 32(1).

[2] Geffen, J. A. v., 1976, "Piercing Tools," U. Patent, ed.

[3] Geffen, J. A. v., 1979, "Method and Apparatuses for Forming by Frictional Heat and Pressure Holes Surrounded Each by a Boss in a Metal Plate or the Wall of a Metal Tube," U. Patent, ed.

[4] Geffen, J. A. v., 1979, "Rotatable Piercing Tools for Forming Holes Surrounded Each by a Boss in Metal Plates or the Wall of Metal Tubes," US Patent.

[5] Mahoney, M. W., 1999, "Friction boring process for aluminium alloys." U. Patent, ed.

[6] Miller, S. F., Blau, P. J., and Shih, A. J., 2007, "Tool wear in friction drilling," International Journal of Machine Tools & Manufacture, 47(10), pp. 1636-1645.

[7] Scott F. Miller ; Rui Li ; Hsin Wang ; McSpadden Jr, S. B. A. J. S., 2006, "Experimental and numerical analysis of the friction drilling process," Journal of Manufacturing Science and Engineering, ASME 128(3).

[8] Flowdrill© , "http://flowdrill.com."

[9] Miller, S. F., Tao, J., and Shih, A. J., 2006, "Friction drilling of cast metals," International Journal of Machine Tools and Manufacture, 46(12-13), pp. 1526-1535.

[10] Demir, Z., and Ozek, C., 2014, "Investigate the Effect of Pre-drilling in Friction Drilling of A7075-T651," Materials and Manufacturing Processes, 29(5), pp. 593-599.

[11] Geffen, J. A. v., 1980, "Rotatable piercing tools for forming bossed holes," US Patent.

[12] Glenn D. Head, J., Louis P. Bredesky, J., Lemaster, W. C., and Winter, D. C., 1984, "Flow drilling process and tool therefore," U. S. Patent, ed.

[13] Hoogenboom, A. J., 1982, "Flow drill for the provision of holes in sheet material." US Patent.

[14] France, J. E., Davison, J. B., and Kirby, P. A., 1999, "Strength and rotational stiffness of simple connections to tubular columns using flowdrill connectors," Journal of Constructional Steel Research, 50(1), pp. 15-34.

[15] France, J. E., Davidson, J. B., and Kirby, P. A., 1999, "Moment-capacity and Rotational Stiffness of Endplate Connections to Concrete-filled Tubular Columns with Flowdrilled Connectors," Journal of Constructional Steel Research, 50, pp. 35-48.

[16] Overy, K., 1978, "Flowdrilling - Bush Formation in Thin Metal," Cme-Chartered Mechanical Engineer, 25(7), pp. 70-75.

[17] Kerkhofs, M., Stappen, M. V., D'Olieslaeger, M., Quaeyhaegens, C., and Stals, L. M., 1994, "The Performance of (Ti,Al)N-coated Flowdrills," Surface and Coatings Technology, 68/69, pp. 741-746.

[18] Sato, N., Terada, O., and Suzuki, H., 1997, "Adhesion of aluminum to WC-Co cemented carbide tools," Funtai Oyobi Fummatsu Yakin/Journal of the Japan Society of Powder and Powder Metallurgy(44(4)), pp. 365-368.

[19] Ozler, L., and Dogru, N., 2013, "An Experimental Investigation of Hole Geometry in Friction Drilling," Materials And Manufacturing Processes, 28(4), pp. 470-475.

[20] Miller, S. F., Blau, P. J., and Shih, A. J., 2005, "Microstructural alterations associated with friction drilling of steel, aluminum, and titanium," Journal Of Materials Engineering And Performance, 14(5), pp. 647-653.

[21] Chow, H.-M., Lee, S.-M., and Yang, L.-D., 2008, "Machining characteristic study of friction drilling on AISI 304 stainless steel," Journal of Materials Processing Technology, 207(1-3), pp. 180-186.

[22] Feng, Z., Santella, M. L., David, S. A., Steel, R. J., Packer, S. M., Pan, T., Kuo, M., and Bhatnagar, R. S., 2005, "Friction Stir Spot Welding of Advanced High-Strength Steels - A Feasibility Study," Society of Automotive Engineers

[23] Chao, Y. J., Qi, X., and Tang, W., 2003, "Heat Transfer in Friction Stir Welding - Experimental and Numerical Studies," Journal of Manufacturing Science and Engineering, 125, pp. 138-145.

[24] Soundararajan, V., Zekovic, S., and Kovacevic, R., 2005, "Thermo-mechanical model with adaptive boundary conditions for friction stir welding of Al 6061," International Journal of Machine Tools & Manufacture, 45, pp. 1577-1587.

[25] Miller, S. F., and Shih, A. J., 2007, "Thermo-Mechanical Finite Element Modeling of the Friction Drilling Process," Journal of Manufacturing Science and Engineering, 129(3).

[26] Raju, B. P., and Swamy, M. K., 2012, "Finite Element Simulation of a Friction Drilling process using Deform-3D," International Journal of Engineering Research and Applications (IJERA), 2(6), pp. 716-721.

[27] ABAQUS, 2013, ABAQUS 6.13 documentation.

[28] Fernández, A., Lacalle, L. N. L. D., and Lamikiz, A., 2010, "Friction drilling of stainless steels pipes," AIP Conference Proceedings, 1315, pp. 1187-1192.

[29] Strenkowskia, J. S., Hsieha, C. C., and Shih, A. J., 2004, "An analytical finite element technique for predicting thrust force and torque in drilling," International Journal of Machine Tools & Manufacture, 44, pp. 1413-1421.

[30] Miller, S. F., Li, R., Wang, H., and Shih, A. J., 2006, "Experimental and numerical analysis of the friction drilling process," Journal of Manufacturing Science and Engineering-Transactions of the Asme, 128(3), pp. 802-810.

[31] Miller, S. F., 2006, "Experimental Analysis and Numerical Modeling of the Friction Drilling Process," Doctor of Philosophy, The University of Michigan.

[32] C.J., D., and W.M., T., 1996, "Friction stir process welds aluminum alloys," Welding Journal, 75(3), pp. 41-45.

[33] Thomas, W. M., Nicholas, E. D., Needham, J. C., Murch, M. G., Temple-Smith, P., and Dawes, C. J., 1991, "Friction stir butt welding," I. Patent, ed.

[34] Nandan, R., DebRoy, T., and Bhadeshia, H. K. D. H., 2008, "Recent advances in friction-stir welding – process, weldment structure and properties," Progress in Materials Science, 53, pp. 980-1023.

[35] Gould, J. E., Lienert, T. J., and Feng, Z., 1998, "Recent developments in friction stir welding," Aerospace Manufacturing Technology Conference & Exposition, SAE Technical Paper Series 981875.

[36] Li, Y., Ngai, T. L., Xia, W., Long, Y., and Zhang, D., 2003, "A study of aluminum bronze adhesion on tools during turning," Journal of Materials Processing Technology, 138, pp. 479-483.

[37] Boopathi, M., Shankar, S., Manikandakumar, S., and Ramesh, R., 2013, "Experimental investigation of friction drilling on brass, aluminium and stainless steel," Procedia Engineering, 64, pp. 1219-1226.